



Cite this: *RSC Adv.*, 2023, **13**, 2036

Received 23rd September 2022  
 Accepted 28th December 2022

DOI: 10.1039/d2ra06004c  
[rsc.li/rsc-advances](http://rsc.li/rsc-advances)

## Towards interactional management for power batteries of electric vehicles

Rong He, <sup>a</sup> Wenlong Xie, <sup>a</sup> Billy Wu, <sup>b</sup> Nigel P. Brandon, <sup>c</sup> Xinhua Liu, <sup>ab</sup> Xinghu Li<sup>a</sup> and Shichun Yang<sup>\*a</sup>

With the ever-growing digitalization and mobility of electric transportation, lithium-ion batteries are facing performance and safety issues with the appearance of new materials and the advance of manufacturing techniques. This paper presents a systematic review of burgeoning multi-scale modelling and design for battery efficiency and safety management. The rise of cloud computing provides a tactical solution on how to efficiently achieve the interactional management and control of power batteries based on the battery system and traffic big data. The potential of selecting adaptive strategies in emerging digital management is covered systematically from principles and modelling, to machine learning. Specifically, multi-scale optimization is expounded in terms of materials, structures, manufacturing and grouping. The progress on modelling, state estimation and management methods is summarized and discussed in detail. Moreover, this review demonstrates the innovative progress of machine learning based data analysis in battery research so far, laying the foundation for future cloud and digital battery management to develop reliable onboard applications.

### 1 Introduction

The automotive industry has experienced rapid development in the past 100 years and brought great convenience to people's lives.<sup>1</sup> However, a global shift to electric vehicles (EVs) is certainly the solution to address increasing environmental concerns,<sup>2</sup> with the development of high energy-density, low cost and durable energy storage systems a key enabler. Early battery technologies for EVs include lead-acid and nickel-metal hydride chemistries, and technologies such as hydrogen fuel cells and supercapacitors have also been explored.<sup>3</sup> However, lithium-ion batteries (LiBs) are the current technology of choice for EVs. Here, common cathode chemistries include lithium cobalt oxide (LCO), lithium manganese oxide (LMO), lithium iron phosphate (LFP), lithium nickel cobalt aluminium oxide (NCA) and lithium nickel–manganese–cobalt oxide (NMC), which offer relatively high energy density, long lifespan and high efficiency compared to other battery chemistries.

Due to the usage dependent degradation and instability of LiBs, outside of certain operating windows, a real-time embedded battery management system (BMS) is of vital importance for maintaining safety and reliability.<sup>4</sup> The key objective of a BMS is to monitor key states, minimize degradation,<sup>5</sup> balance cells<sup>6</sup> and detect faults.<sup>7</sup> Research and development in LiBs have traditionally focused on electrode and electrolyte development across multiple length scales,<sup>8</sup> however linking these insights into the design of BMSs remains an urgent need.<sup>9</sup> State of charge (SOC)<sup>10</sup> is one of the key states and indicates the remaining capacity in a cell, whereas state of



*Professor Yang Shichun is Dean of School of Transportation Science & Engineering at Beihang University, Leading personnel of scientific and technological innovation in the National Ten-thousand Talents Program, leading personnel among the young and middle-aged in the Ministry of Science and Technology. Vice Chairman of Electric Vehicle Division of National Technical Committee of Automobile Standardization (NTCAS), expert of Road Vehicle Specialized Committee of China Intelligent Transportation System Association (CTTSA), Vice Chairman of SAE Vehicle Safety and Information Security Technical Committee. His research mainly works on scientific and technological research for EV power system safety, high-efficient optimal theory and integrated control.*

Open Access Article. Published on 11 January 2023. Downloaded on 1/13/2026 4:14:31 AM.  
 This article is licensed under a Creative Commons Attribution-NonCommercial 3.0 Unported Licence.

health (SOH) indicates the remaining useful lifetime of the battery. In many cases, an accurate model of the battery is needed to estimate these states and how they evolve with common examples being the estimation of capacity, available power,<sup>11</sup> and remaining energy.<sup>12</sup> Model exist at different levels of complexity but multi-scale models<sup>13</sup> provide a deeper insight into battery performance allowing for more intelligent and accurate performance prediction.

With the advent of the Internet-of-Things (IoT)<sup>14</sup> era, the potential to fuse recent developments into cloud-enabled BMSs has the potential to create a new revolution in intelligent EV management.<sup>15</sup> In this scenario, the communication, computation and control, of the batteries, is distributed to the cloud and physical devices mostly act as data collectors. This enhances the scalability, cost-effectiveness, adaptability, and flexibility of the systems. Although the actual cloud-based battery condition monitoring for energy storage systems has been less applied, the potential benefits of advancing the BMS has wide acknowledgement.<sup>16</sup> Cyber-physical systems (CPS), which fuse real-time sensing data with advanced models, therefore, is seen as the future of BMSs with core elements including cloud data storage, intelligent analytics, advanced control algorithms, and data visualization.<sup>10</sup>

Motivated by the potential of new digital solutions towards advancing BMSs this paper is organized as follows. Section 2 presents a framework: the cyber hierarchy and interactional network (CHAIN) proposed for data fusion with models and intelligent control. In Section 3, key considerations for the management of LiBs are discussed, starting from atomic considerations and increasing up to pack and system-level challenges. Modelling methods and state estimation techniques are discussed along with the latest developments in BMSs in Section 4. Section 5 reviews the artificial intelligence (AI) methodologies for data analysis that are being considered for promising BMS application. Section 6, then focuses on typical applications and innovative BMS developments and the last section offers perspectives and highlights challenges for further research in the field of intelligent BMSs.

## 2 CHAIN: battery management framework

With the coming of the data-driven era, IoT, big data, service-oriented technology,<sup>17</sup> and cloud computing,<sup>18</sup> have presented new pattern to do scientific research. Countries are simultaneously setting up data centres to accelerate the research through cloud-managed data sets such as high-energy physics, genomics, meteorology and ocean earthquakes.<sup>19</sup>

The traditional BMSs are severely restricted by onboard computing power and memory due to the relatively high costs of software and hardware.<sup>20</sup> With the advent of IoT devices, it is expected that data processing with high real-time requirements can be moved to the cloud through wireless communication for control strategies feedback by large calculated data-driven approaches.<sup>21</sup> The BMS at the vehicle-end focuses on collecting sensor data and completing data communication and

interaction with the cloud. With this in mind, Yang *et al.*<sup>22</sup> provides the CHAIN framework, which consists of the distributed structure of vehicle-end and cyber-end as shown in Fig. 1. By transferring the computing load of the vehicle-end BMS, we can give play to the potential of cloud computing and storage, and build a multi-scale model of the battery. And then, as shown in Fig. 2, an overall framework utilizing an end-edge-cloud architecture for a cloud-based BMS is proposed, with the composition and function of each link described, which leverages from the CHAIN framework.<sup>23</sup> Data collected by the sensor at the vehicle-end is encrypted and uploaded, which is one of the emerging challenges for IoT enabled devices.<sup>24</sup> After cloud physical model fusion or machine learning calculation, the updated decision results are fed back to the vehicle in real time for performance optimization. Hierarchical management including real-time monitoring, communication, analysis, and decision serve the vehicle greater efficiency, safety and predictability. The digitalized services are inseparable from the collection, transmission, storage, computation and analysis of scientific data, resulting in final decision making.<sup>25</sup> Alam *et al.*<sup>230</sup> presented a vehicular application for cloud-based CPS containing three operational modes that have analytically modelled the computation, communication and control properties and provides optimized control decisions based on system-wide information collection.

With aggregated data in the cloud, physical models can estimate immeasurable states to gain deeper insights towards better decisions. The demands of collecting EV data creates an unprecedented opportunity for novel information exchange ways.<sup>26</sup> Smart cars based on big data are an important strategic direction for the transformation and progression of the automotive industry and sustainable development. It is no doubt that a precise mathematical model for LiB that applies to the characteristics of big data is therefore needed.<sup>27</sup> Successful applications of this approach to real-world problems have included: optimization of shared charging infrastructure<sup>28</sup> and shared EVs.<sup>29</sup> Therefore, how to generate, combine and use data

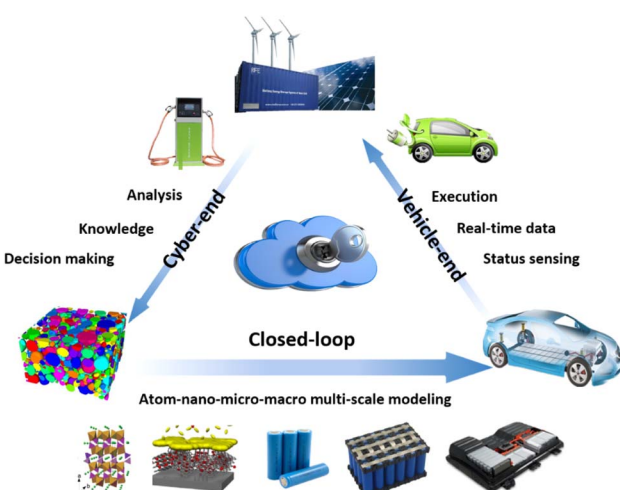


Fig. 1 CHAIN management framework.<sup>22</sup>



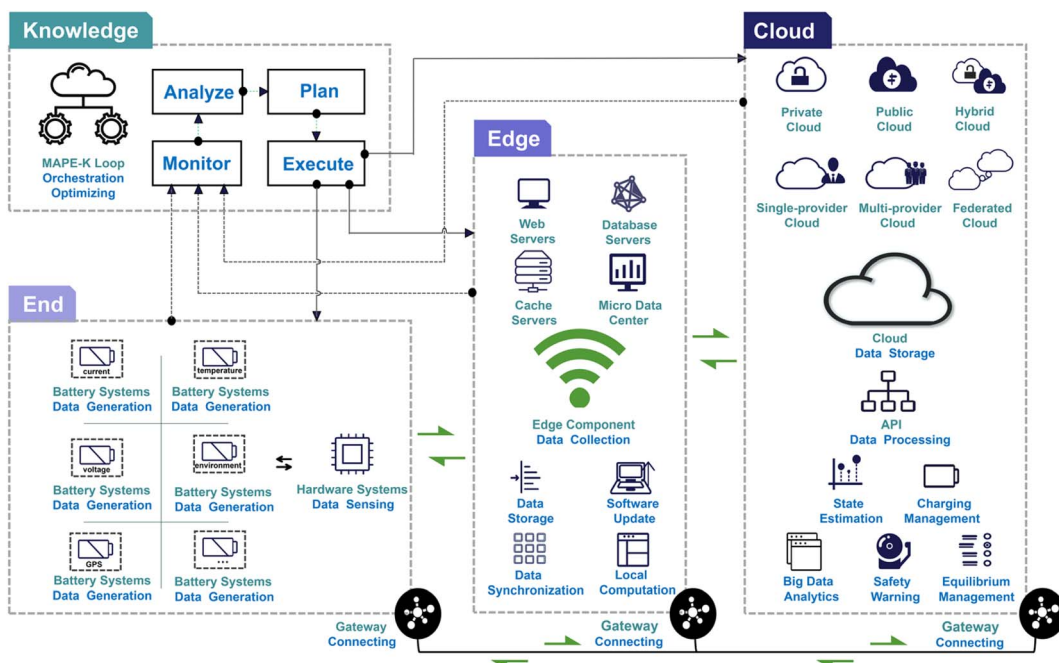


Fig. 2 A cloud to things framework, which consists of four subsystems: end, edge, cloud and knowledge.

in CPSs for better vehicle durability requires intelligent analysis implemented for online BMS.<sup>30</sup> The relevant technology barriers must be reduced to make analytical tools more accessible and to improve data and visualization literacy.<sup>31</sup>

### 3 Physical multi-scale research for battery

With databases, the core task of an interactive system is model-based analysis. A combination of mathematical descriptions of the physical processes occurring in the battery and experimental parameterization of the model constants is needed to model the dynamic behaviour of the battery.<sup>32,33</sup> To understand how key information propagates between length scales, it is necessary to describe key aspects of this from fundamental materials, then to manufacturing and cell leveller performance, and finally to the module and system considerations.

#### 3.1 Materials

The operating principle of a LiB is underpinned by the redox reactions and the electrochemical potential in the electrode active materials.<sup>34</sup> This involves the movement of ions and electrons, which in turn allow for the storage/delivery of electrical energy.<sup>35</sup> The cations move between the anode and cathode through the electrolyte, while electrons flow through conductive agents and current collectors in the cell to the external circuit where useful electrical work can be extracted.<sup>36</sup> At present, widely adopted electrode materials exist for LiBs, with different strengths and weaknesses as shown in Table 1.

Extensive research has been performed in recent years covering the cost and performance of battery materials. The

multi-physical and multi-scale in nature increase the complexity for seeking promising materials, which can be settled by model. As an example, it found that mechanical failure of anode electrodes is highly strain-rate dependent with the help of a computational model.<sup>37</sup> Similarly, a multi-physics and multi-scale model approach for analyzing Si-C composite anodes can be used to optimize the effects of different Si loadings, mechanical constraints and charging rate in terms of electrochemical and mechanical performance.<sup>38</sup> Other models, such as parametric stochastic microstructure models, have been used to investigate the influence of microstructure. Here good correlation was found between the virtually generated cathodes and the morphological properties of the 3D tomographic image data, opening up the possibility of *in silico* design.<sup>39</sup> These microstructural models, highlight the importance of capturing geometric complexities and, thus, there has been a general trend to improve the accuracy of physics-based models by including the heterogeneity of the porous electrode structure.<sup>40</sup>

In terms of safety, internal failures caused by loss of electrode materials, structure deformation and dendrite growth are also preventable through material design.<sup>41</sup> Cathode particles with carbon coatings have better electronic conductivity often exhibit high coulombic efficiency on LFP.<sup>42</sup> Surely graphite is stable relative to organic electrolytes when delithiated or at high voltages relative to lithium. Thick electrodes focus on low tortuosity structural designs for rapid charge transport and high energy density, cell stability, and durability.<sup>43</sup> So far, electrode thickness is contradictory to the mechanical stability and electrode conductivity.<sup>44</sup>

In addition to the electrodes, the electrolyte responsible for ionic transport, also significantly affects the battery

Table 1 Comparison of electrodes' materials

Electrodes	Materials	Strengths	Weaknesses
Cathode	LCO	120–150 W h kg <sup>−1</sup> High energy/power	Thermally unstable Lower cycle life Limited load capabilities
	LMO	105–120 W h kg <sup>−1</sup> Enhanced thermal stability Low cost	Low capacity Limited cycle life
	NCA	80–220 W h kg <sup>−1</sup> High specific energy/power Long cycle life	Safety issues Cost
	NMC	140–180 W h kg <sup>−1</sup> High specific energy/power Low internal resistance	Low stability Low specific energy
	LFP	80–130 W h kg <sup>−1</sup> Inherently safe Acceptable thermal stability High current rating Long cycle life	Lower energy density
Anode	Graphite/carbon-based	High mechanical stability Conductivity and Li-ion transport Gravimetric capacity	Low gravimetric capacity
	LTO	High charge/discharge rates Inherently safe Long cycle life	Lower energy density Cost
	Si	Gravimetric/volumetric capacity Chemical stability Low cost	High degree of mechanical expansion on charging

performance. By means of a mathematical model, it is found that poor lithium-ion mobility causes depleted zones regions in electrodes as the porosity decreases or the length of the separator increases.<sup>45</sup> This transport phenomenon is also stress coupled. In another work, a coupled ionic conduction-deformation model for a solid polymer electrolyte was developed to investigate the effect of mechanical stresses induced by the redistribution of ions. They found that externally applied stresses can reduce the concentration gradient of ions across the electrolyte thickness and prevent salt depletion at the electrode–current collector interface.<sup>46</sup>

The separator is placed between the cathode and anode to prevent physical contact with the electrodes while facilitating free ionic transport and electronic isolation. The main characteristics that affect the performance of the separator consist of permeability, porosity, as well as chemical, mechanical and thermal stability.<sup>47</sup> Specifically, mechanical behaviour and ionic conductance of the separator under compression influences the battery thermal performance. In the literature, the separator has been modelled as an open-cell foam to describe the mechanical deformation under compressive loads and the resulting ionic conductivity.<sup>48</sup> Xu *et al.*<sup>49</sup> developed a micro-structure-based modelling method to predict the mechanical behaviour of LiBs separators. The proposed method successfully captures the anisotropic behaviour of the separator under tensile tests and provides insights into the microstructural deformation, such as the growth of voids.

With the increasing abundance of test data, fresh avenues based on big data is promising for battery modelling to

optimize material properties. Sendek *et al.*,<sup>50</sup> for instance, presented a new type of large-scale computational screening approach for identifying promising candidate materials for solid-state electrolytes for LiBs that is capable of screening all known lithium-containing solids. The screening reduces the list of candidate materials from 12 831 down to 21 structures that show promise as electrolytes, few of which have been examined experimentally. With large databases, data screening can be conducted to obtain high conductivity, robust, and low-cost materials for batteries.

### 3.2 Manufacturing

The cost and performance of the battery are inseparable from the manufacturing process. Raw materials are the most expensive component, while the second one is electrode manufacturing, which affects performance metrics such as energy density.<sup>51</sup> The incentive for improving electrode manufacturing lies largely in the ability to significantly increase the volume ratio of active materials, resulting in higher energy density and lower cost.<sup>52</sup>

The electrode manufacturing process is shown in Fig. 3. The active material, conductive additive, binder and other components are mixed in a solvent. The capacity and energy, electronic conductivity and mechanical integrity of the electrode are determined by these ingredients. The mass ratios between the ingredients must be such that the optimal combination of properties is attained.<sup>53</sup> Moreover, the selection of the solvent will determine which binders are suitable and whether additional additives will be required.<sup>54</sup> The resulting suspension,



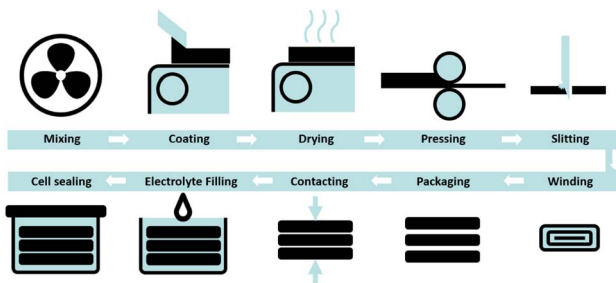


Fig. 3 The electrode manufacturing process.

which is referred to as the electrode slurry, is then coated onto a metal foil.<sup>55</sup> In the laboratory, comparatively primitive equipment coating such as the doctor blade is usually used to achieve the coating, while the slot-die coater is used at the industrial level. Surface coating can improve the interface properties, cycle-life, rate performance and stability of cathode materials for LiBs.<sup>56</sup> After the coating is dried, it will be compressed down to the desired thickness in the next pressing step. The remaining stages are electrode slitting, winding, packaging, contacting, electrolyte filling, and cell sealing.

The manufacturing process modelling is also effective means to improve battery performance. Chouchane *et al.*<sup>57</sup> reported a novel computational simulation of NMC electrode performance for different compositions, which explicitly consider the three-dimensional of the active material. The impact of slight variations in the electrode manufacturing model can link electrode properties such as variations in thickness, electrode density and active material weight fraction with the performance of battery modules made from these cells.<sup>58</sup> Optimum whole-cell design in terms of simultaneous optimization of electrode thicknesses, volume fractions of porosity and total solids and specific cell mass are designed for enhancing total charging times.<sup>59</sup>

In the production of LiBs, electrode production, cell production and cell conditioning contribute similarly to the total manufacturing cost. For the cost models, there is a particular need to predict new technologies (Li-air, Li-S, *etc.*) based on technical parameters, *e.g.* using process-based cost modelling techniques.<sup>60</sup> Compared with conventional 2D planar structures, hierarchical 3D structures<sup>61</sup> can yield shorter diffusion pathways and lower resistance during the ion-transport process, as well as providing increased energy density by creating porous structures with larger surface areas that can improve electrode reaction and ion transfer while efficiently using the limited space in a compact battery.<sup>62</sup> By tuning synthesis conditions (*e.g.* temperature and atmosphere), nano-materials with desirable structures and properties can be obtained, leading to various usage areas for energy storage and conversion applications (*e.g.* batteries, supercapacitors and catalysts).<sup>63</sup>

To monitor internal temperature for safety purposes, multi-point thin-film sensors have been integrated into the LiBs electrodes, that retain a stable capacity with high coulombic efficiency over 100 cycles.<sup>64</sup> In the case of battery combustion

and explosions, the highly flammable liquid electrolyte serves as the “fuel”. Thus, the separators and liquid electrolytes are two key components that need improvements.<sup>65</sup>

### 3.3 Cell

The cell is the smallest unit in BMS research to predict and control the overall cycling performance of the module and pack. This section will briefly introduce the principle of cell modelling. For more details, please refer to Section 4.

LiBs electrodes are usually made from large amounts of active material and conductive material particles. In the assembly, the active substance and conducting agent particles constitute a porous solid network, while the liquid electrolyte occupies the internal pore space. Porous electrode theory allows for a detailed description of the electrochemical processes occurring in the battery which determines its performance. On this account, Newman *et al.*<sup>66</sup> proposed a multi-domain electrode model in which the electrode area is divided into two phases: a solid phase to represent the active material, and a liquid electrolyte phase. The main advantage of the porous electrode is that it has a large electrochemically active surface area which facilitates high power performance.<sup>67</sup> The current and reaction distributions through the depth of the electrode are strongly influenced by the type of activation polarization and by mass transport of the reacting ionic species, in addition to the effective conductivities of the two phases.<sup>68</sup> The main advantage of the porous electrode is that it has a large electrochemically active surface area which facilitates high power performance.<sup>67</sup> The current and reaction distributions through the depth of the electrode are strongly influenced by the type of activation polarization and by mass transport of the reacting ionic species, in addition to the effective conductivities of the two phases.<sup>68</sup>

The gap between macroscopic (operating conditions) and microscopic (aging mechanism) can be well bridged by the proper models. Constitutive models are widely used to account for complex chemical and physical processes taking place inside the battery, such as side reactions. It was found that the side reactions lead to the deposit forming the overgrowth of solid-electrolyte interphase (SEI) on the graphite and produce an apparent deposited layer (lithium plating) on the anode particle surface.<sup>69</sup> To characterize electrode behaviours by mechanical-electrochemical factors and establish constitutive models for electrodes can be utilized as degradation representatives to explicitly quantify the aging effects.<sup>70</sup>

High currents increase the probability of metallic lithium microstructures forming, raising safety concerns due to (internal short circuit) ISC and subsequent catastrophic failure.<sup>71</sup> In addition to forming metallic structures, lithium is known to react in environments containing electrolytes and solvents, irreversibly forming lithium-organic salt deposits. It remains of fundamental interest to directly image the growth processes involved to understand their formation and prevent it. Arora *et al.*<sup>72</sup> firstly described the conditions for lithium deposition during overcharge. They extended Doyle's model<sup>73</sup> with a side reaction described by a Butler-Volmer equation on



the negative electrode and investigated lithium deposition under various operating conditions, with various cell designs and charging protocols. The cell capacity loss is mostly due to the loss of lithium (LLI).<sup>74</sup> Indicators for plating were collected by electrical stripping measurements as well as optical and laser microscopy measurements on fully charged disassembled cells. A novel method of using voltage plateau end-point gradients enables the measurement of lower levels of lithium stripping and plating.<sup>75</sup> While all cells that show indications of plating in the electrical measurements also showed indications of plating in the optical analysis, the reverse conclusion is not valid.<sup>76</sup> It is widely believed that Li plating can be detected and quantified by using a minimum in differential voltage signal. Whereas, the model proposed by O'Kane predicts that the minimum is a shifted and more abrupt that cannot be used to quantify stripping.<sup>77</sup> Baker *et al.* proposed a Li activity model wherein the activity of plated lithium differs from the activity of bulk Li.<sup>78</sup> Besides, tab design correlates to Li-plating at high-rate constant-current charging.<sup>79</sup>

Many researchers have argued that the most important LiBs degradation mechanisms are the passivation layer on the graphite electrode. The cycled cell is likely to experience an initially faster rate of SEI growth compared to the cell held at constant potential due to the exposure of the electrode to the electrolyte as a result of cracks caused by cycling.<sup>80</sup> Moreover, dendrite growth stretches the SEI and changes the curvature of the SEI layer, affecting the SEI evolution. Accordingly, SEI growth changes the resistance and reaction current, evolving dendrite morphology.<sup>81</sup> During the initial charging, an electric double layer forms at the electrode/electrolyte interface due to the self-assembly of solvent molecules before any interphase chemistry occurs.<sup>82</sup> Liu developed a coupled dendrite and SEI growth model that has been used to investigate the impact of applied current density, SEI resistivity and SEI defects/inhomogeneity on dendrite formation and growth. SEI grows more quickly during charge than discharge due to the difference in electron flux through the SEI layer and the temperature change during cycling. A non-destructive method based on the electromotive force derivative analyses identifies the degradation mechanisms of the individual electrodes.<sup>84</sup> Both the SEI formation at the anode and anode degradation have been experimentally confirmed. Horstmann *et al.*<sup>85</sup> and Single *et al.*<sup>86</sup> draw an overview of multi-scale models for SEI growth. Das *et al.* proposed a detailed kinetically limited SEI growth model with spatially resolved concentrations.<sup>87</sup> But most authors use a kinetically limited SEI growth model using a Tafel equation, with the exchange current density as a fitting constant.

#### 3.4 Module and system

The cell-scale research mainly focuses on performance, while the module and system pay attention to management applications in EVs. There have been many approaches proposed for the management of single cells, the control of module and pack are less investigated and usually relies on simplified methods.

The current distributions variations, voltage imbalance, interconnection resistances and thermal gradients in packs,

which leads to impaired performance of the whole energy-storage system. Temperature gradient during cycling led to differing degradation rates, whereas the colder cells showed aggravated aging behaviour.<sup>88</sup> In addition, interconnect resistances in parallel can cause the current heterogeneity that can be further influenced by the cell temperature.<sup>89</sup> Different laminate design schemes will result in different hazard patterns. A larger layer number will delay the thermal runaway of the battery, but increase the seriousness of thermal hazard.<sup>90</sup> To reduce the computational cost, a sensitivity-based model predictive control formulation is proposed that makes optimal model-based control suitable for real-time implementation on a battery pack composed of dozens of cells.<sup>91</sup>

The adaption of different joining technologies greatly influences the central characteristics of the packs in terms of battery performance, capacity and lifetime. The most common joining techniques are ultrasonic welding, wire bonding, force fitting, soldering, laser beam welding, and resistance welding, as well as friction stir welding, tungsten inert gas welding, joining by forming and adhesive bonding.<sup>92</sup>

## 4 Digital management for battery

The development of communication transmission technology and the research of internet applications have promoted the collaborative integration of the cyber-end and vehicle-end for an interconnected, self-reconfigurable BMS involving clouded communication and computing integrated, as shown in Fig. 4. The BMSs in the vehicle-end collect enormous datasets for various battery materials, grouping styles throughout real-time monitoring, encrypt and upload to the cyber-end simultaneously. The cyber-BMS has lifecycle management methods for states state estimation, safety and fault prognosis and thermal management.

### 4.1 Battery modelling

Over the last decades, lots of efforts have been taken to work on models for state prediction and performance optimization. The common categories of models are equivalent circuit model<sup>93</sup> and electrochemical models.<sup>94</sup> There are also some multi-physics coupling models such as the electro-thermal-mechanical coupling model. The thermal issues have usually been coupled with models parameters focusing on performance degradation even thermal runaway due to dynamic loading.<sup>95</sup>

**4.1.1 Equivalent circuit model.** As the semi-mechanical grey-box model, ECM abstracts away the electrochemical nature of the battery and represent it solely as electrical components. ECMs replicate the volt-ampere dynamics of the battery by composed of several resistors, capacitors and Warburg elements in series and parallel.<sup>96</sup> All the circuit components are expressed as explicit functions of the state and input variables, which are parameterized by fitting the cell voltage response with the algorithm.<sup>97</sup> Owing to easily calculation and analysis, they are widely employed for module and system modelling closely to the real complex working condition in BMS simulation and applications.<sup>98</sup>



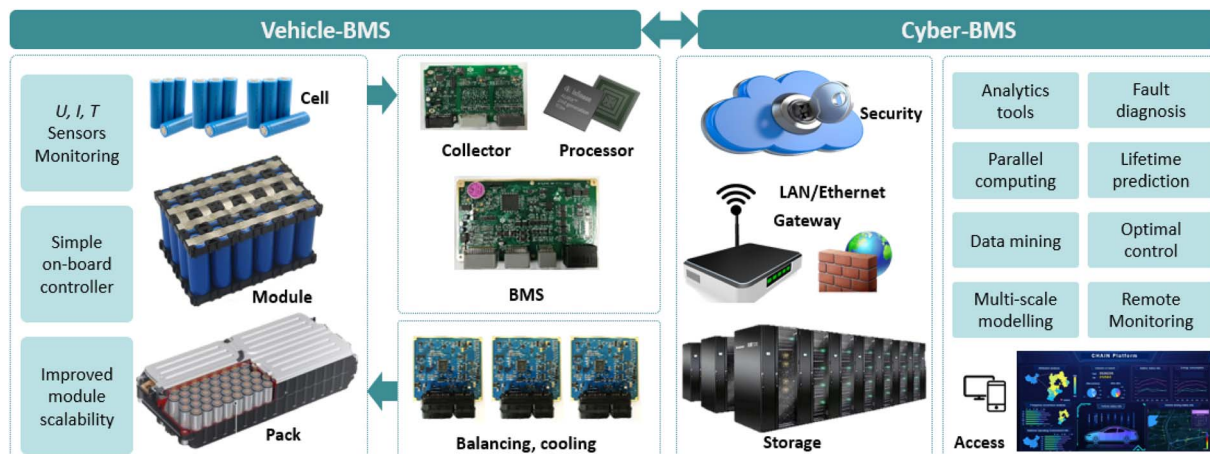


Fig. 4 The framework of interconnected and self-reconfigurable BMS.

On account of the strong nonlinear relationship between OCV and SOC, the OCV–SOC fitting and modelling is needed.<sup>99</sup> ECM considering thermal is also common to capture the heat propagation from the cells through the entire pack and to the environment.<sup>100</sup> To study the physico-chemical properties and the causes of the change with model parameters over the battery lifetime, ECMs allows the characterization of electrochemical systems in the frequency domain, which is one of the most accurate techniques for decoupling the dynamics in frequency and spatial domain studying and diagnosis of electrochemical behaviour.<sup>101</sup> By means of electrochemical impedance spectroscopy (EIS),<sup>102</sup> frequency-dependent impedance fluctuations can be monitored during charging and discharging sequences of the battery according to the resonant frequency of the circuit.<sup>103</sup> The individual contribution quantification for different loss mechanisms can be identified by their parameter dependencies in the frequency domain.<sup>104</sup>

**4.1.2 Electrochemical model.** Electrochemical models simulate the LiBs' internal characteristics and reactions according to chemical/electrochemical kinetics and transport equations, which consist of a set of coupled partial differential equations, explaining how the potential is produced and affected by the electrochemical reactions taking place in the battery.

In pseudo-two-dimensional (P2D), the lithium transports from the anode through the separator into the cathode are modelled macroscopically based on the concentrated solution theory. While the kinetics of lithium diffusion inside the cathode particles are simplified along the radius direction for the symmetry of the spherical particles.<sup>105</sup> As shown in Fig. 5, (1) the solid-state  $\text{Li}^+$  ions concentration  $c_s$  in the electrodes is derived from Fick's law of diffusion for spherical particles; (2) the liquid-phase  $\text{Li}^+$  ions concentration  $c_e$  in the electrolyte and the separator is based on the conservation of  $\text{Li}^+$  ions; (3) the solid-state potential  $F_s$  in the electrodes is derived from Ohm's law; (4) the liquid-phase potential  $F_e$  in the electrolyte and the separator is calculated using Kirchhoff's and

Ohm's laws; (5) the pore wall flux of  $\text{Li}^+$  ions  $J$  in the electrodes is described by the Butler–Volmer kinetics equation.

By modifying two boundary conditions of the original P2D model, the effective electrical conductivity of the separator is a crucial parameter describing the micro ISC severity, as well as fault diagnosis and battery design.<sup>106</sup> The original electrochemical model can be reformulated by lumped parameters to produce a full-order model with the number of parameters reduced from 36 down to 24, which making system identification possible.<sup>107</sup> However, the complexity makes more need of memory and computational effort, which goes against the fast computation and real-time implementation for BMS. As a solution, reduced-order models predict the cell response with varying degrees of fidelity and model complexity by discretization techniques that can be applied to retain only the most significant dynamics of the full order model. The proper orthogonal decomposition and discrete empirical interpolation method for model order reduction are convenient for real-time applications.<sup>108</sup>

To reduce the computational times, a simplified version, single particle model (SPM)<sup>109</sup> has two basic assumptions: first,

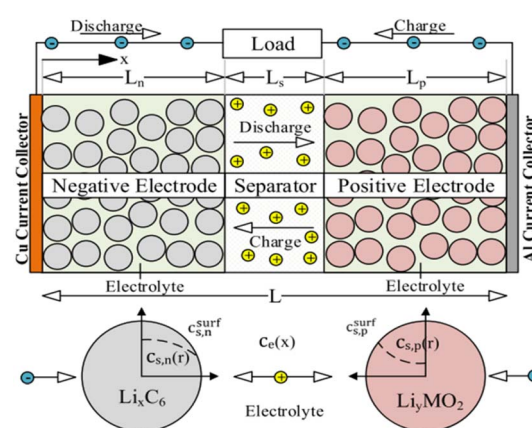


Fig. 5 Schematic of SPM and P2D model.



each electrode is modelled as two spherical particles in which intercalation and de-intercalation phenomena occur. Second, the variations in the electrolyte concentration and the potential are ignored. SPM could also be simplified using the three-parameter polynomial approximation method and the volume-average integration method. Then, a parabolic profile is utilized to approximate the concentration within each spherical particle of both electrodes. Advanced SPM with electrolyte physics comprehensively coupling between mechanical and chemical battery degradation presented accurate and fast SOH estimation for BMS.<sup>110</sup>

Except for the material properties of the battery electrodes, the influences of the micro-scale morphological features on the local lithium concentration distribution, electric potential and macroscopic discharge performance can be simulated by the lattice Boltzmann method,<sup>111</sup> which is more convenient in geometry and more efficient in the calculation to solve the governing equations and predict the ion and electron transport within porous electrodes.<sup>112</sup>

Though the battery processes are described in detail in electrochemical models, making them the most accurate of battery models, the computational complexity is also increased accordingly. It may take hours to simulate a charge–discharge cycle of a detailed battery model if no model reduction approach is used to treat the battery equations.

**4.1.3 Thermal coupled model.** The thermal component of the battery model is essential because the battery major weakness is sensitivity to the temperature that their safety and aging strongly depend on.<sup>113</sup> LiBs heat generation is one of the major phenomena occurs in the battery during cell operating condition that is during charge transport, chemical reaction, discharge and it causes serious temperature changes,<sup>114</sup> especially the thermal runaway for the condition of a low SOC.<sup>115</sup> An efficient thermal model on the understanding the battery build composition dictates the proper selection of expressions that governs the operation of cell such energy balance equations, heat generation equation and boundary condition equation.<sup>116</sup> After Bernardi *et al.* declared the first thermal model for an electrochemical cell, the Bernardi–Newman theory was built on an electrochemical description of diffusion dynamics, charge transfer kinetics and thermodynamics of a battery which can predict the thermal or electrical response. This has been called electrochemical-thermal modelling, which coupled with electrochemical kinetics, charge conservation, mass transport and heat transfer to construct the thermal model within the battery. The parameters generally include the reaction rate, and entropy change, ionic conductivity in the electrolyte and the diffusion coefficient in the electrode and electrolyte.<sup>117</sup> The integrated electro-thermal model is capable of predicting the thermal behaviour and estimating the voltages and temperatures under uncertainties based only on its current and ambient conditions.<sup>118</sup>

The thermal models are typically described based on the degree of their dimensionality. The zero-dimensional or lumped thermal model treat the cell as a lumped mass,<sup>119</sup> while the 3D thermal modelling with the multi-scale and multi-domain framework is demonstrated to be a powerful method to

quantitatively predict thermal behaviours and aid the design of cooling systems for LiBs pack.<sup>120</sup> The thermal-dependent model has the advantage in the real-time prediction of temperature, analysis of large battery pack and development of control strategy.<sup>121</sup> The relationship between the cell energy density and the ease of implementation for the thermal management system is quantified for the first time through varying the cell thickness.<sup>122</sup>

Since the molar volume of the solid phase active material of the battery will change with the lithium intercalation, the concentration gradient will cause certain stress in the material.<sup>123</sup> The mechanical stress experienced by anode, cathode and separator results in thickness and porosity changes in each layer which in turn influences electrochemical behaviour and increase ionic or electronic resistance due to the failure of structural integrity.<sup>124</sup> Liu *et al.* first summarized evolutionary processes under mechanical abuse conditions to classify four processes: mechanical deformation phase, ISC phase, thermal runaway phase, and explosion/fire phase.<sup>125</sup> Laresgoiti's model for surface cracking gives a constant degradation trend because the stress is not affected by previous crack growth.<sup>126</sup> Evolution of temperature and porosity dependent transport properties can be tracked during deformation and layers with higher mechanical strength will suffer low porosity reduction and less susceptible degradation in transport properties.<sup>127</sup>

## 4.2 State estimation on a multi-time scale

The current fluctuations and temperature changes under driving conditions threaten electrochemical reactions in the battery. The data measured by the sensor on the BMS, such as temperature, voltage, and current, can only reflect the external characteristics of the battery system and is not enough to characterize the real-time state inside the battery. In order to avoid the potential safety hazards and ensure reliable operation of the battery system, BMS is expected to be characterized by high accuracy and strong robustness state estimation, which is a research hotspot for nearly a decade.

State estimation is a method to estimate the unknown state of dynamic system based on external measurable data. The data obtained by measuring the input and output of the system can only reflect the external characteristics of the system, while the dynamic performance of the system needs state variables to describe, such as residual power and health. Therefore, state estimation is of great significance for understanding and controlling systems. Accurately estimating the battery state of charge and health can realize reasonable utilization of energy, prevent overcharge, discharge and other safety problems, and extend the service life of the battery. Accurate prediction of the battery performance subsequently allows for efficient digital cloud management systems to be developed.<sup>128</sup> On account of increasingly stringent regulations on safety and performance, battery state estimation features salient cyber-physical design and multi-disciplinary nature by means of the multithread condition monitoring and estimation algorithms.<sup>129,130</sup> As shown in Fig. 6, the measurement of basic parameters includes temperature, voltage and current of battery, to regulate safety



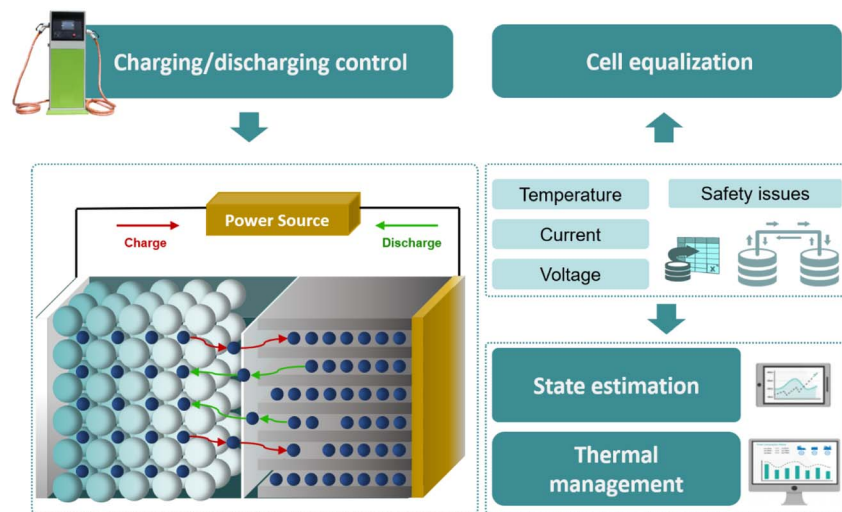


Fig. 6 The main functions of the BMS state estimation algorithm framework.

alarm and avoid potential over-charging/discharging, as well as charging, equalization, state estimation and thermal management. The battery system of electric vehicles is usually consists of thousands of single cells in series and parallel. The electrochemical reactions in charging and discharging process are complex and affected by many factors. The narrow area in which LiBs operate with safety and reliability necessitates effective control and management.

**4.2.1 SOC estimation.** The SOC was put forward by the United States Advanced Battery Consortium (USABC), which gives the remaining capacity of the battery relative to the maximum available capacity that can be released.<sup>131</sup> It is presented as a percentage and cannot be directly measured.

At present, there are four main categories of SOC estimation methods proposed by researchers. The discharge test method is the most reliable, simple and accurate, but it can only be used in the laboratory and needs a given discharging rate. Look-up tables<sup>132</sup> are forthright and accessible, enabling SOC estimation by a consistent one-to-one match between OCV or impedance and the SOC. But the precise table requires enough resting time for the reliability of the internal electrochemistry, which is not suitable for online and precise estimation of SOC.<sup>133</sup> Moreover, OCV is different from terminal voltage and will drift with the service life of batteries.<sup>134</sup> Experiments show that the OCV after discharging and charging at the same SOC always has a voltage interval. Ampere-hour integral method is the most prevalent in applications. In addition to the accuracy of the initial SOC, cumulative deviations of capacity will inevitably occur from measured current integration. Moreover, the operating conditions of the battery including temperature and aging have a great influence on the coulomb efficiency, similarly increasing the cumulative effect of SOC error.

The most studied and promising applications are the ECM-based methods to establish the battery state equations based on the first- or second- order model, which can usually be loosely clustered into filters,<sup>135</sup> observers, and learning algorithms. The filters (e.g., EKF,<sup>136</sup> UKF<sup>137</sup>) achieve the optimal

estimation by adjusting the parameters, avoiding the error accumulation of ampere-hour integral and sensitivity to the error of initial SOC.<sup>138</sup> However, the calculation burden and error is inevitable in the linearization process.<sup>139</sup> The observer (e.g., the Luenberger, H-infinity) method can improve SOC estimation accuracy and robustness, but the performance of the method is easily destroyed by system noise. An adaptive H-infinity filter can cope with the uncertainty of model errors and prior noise evaluation.<sup>140</sup> Owing to the intricate electrochemical behaviour under complex conditions, model selection and parameter acquisition needs the compromise amongst simplicity and accuracy.<sup>141</sup> The error can be less than 5% considering the extreme temperatures and dynamic conditions.<sup>142</sup> Considering OCV aging,<sup>143</sup> hysteresis,<sup>98</sup> noise adaptive,<sup>144</sup> etc. will be more effective in improving accuracy under 1%. For statistical data-driven approaches, please refer to Section 5.

There are three main technological challenges to the progress of SOC estimation.<sup>145</sup> The first is the multi-scale nature of the LiB structure which is nonlinear for modelling accurately, as mentioned in Section 3. Not to mention parameters changes as the battery ages. Second, the internal environment is fluctuating and unpredictable under the dynamic operating conditions (e.g., driving style and charging behaviour) impacting on temperature, C-rate, and SoC range. Finally, the cell heterogeneity directly reduces the performance of the LiB pack system.<sup>146</sup> Most of the estimation measures designed for cell are inappropriate on large-scale modules or pack. Therefore, advanced SoC methods are desiderata required to solve these challenges.

**4.2.2 SOH prediction.** LiBs irrevocably suffer from performance degradation over time (calendar aging) and use (cycle aging) resulting from internal side reactions such as changes of crystal structure, morphology, elemental composition, and electrochemical properties.<sup>147</sup> A wide variety of stresses contribute to degradation including temperature, SOC, charging/discharging rate and depth of charge. Calendar and periodic aging of the battery system throughout the vehicle's



lifecycle, resulting in reduced performance and range. Therefore, the study of battery aging can be as small as the atomic-level microscopic on the physical scale and as large as the macroscopic scale of the power and endurance needs of electric vehicles. Both the analysis of the degradation and the estimation of SOH have developed into research hotspots and inseparable from each other. The success of SOH prediction depends on how well the aging processes and their reasons are understood and mathematically translated from measured data, as well as a degradation model that contributes with key know-how in the design of any application integrating energy storage system (ESS) devices based on LiBs.<sup>148</sup>

SOH refers to the ratio of the present characterization parameters (*e.g.*, capacity, impedance) to that of which when they are not used.<sup>149</sup> There are generally two definitions to quantify battery SOH shown in eqn (1) and (2). Eqn (1) indicates battery energy capability, which is often applied to EVs, PV and ESS where energy storage capacity outweighs power capability. Eqn (2) presents power capability, which is more advantageous in hybrid electric vehicle (HEV) applications.

$$\text{SOH}_E = \frac{C_{\text{current}}}{C_{\text{fresh}}} \times 100\% \quad (1)$$

$$\text{SOH}_P = \frac{R_{\text{EOL}} - R_{\text{current}}}{R_{\text{EOL}} - R_{\text{fresh}}} \times 100\% \quad (2)$$

where  $C_{\text{current}}$  and  $R_{\text{current}}$  are the maximum available capacity and internal resistance during aging,  $C_{\text{fresh}}$  and  $R_{\text{fresh}}$  are the nominal capacity and internal resistance when the battery is in the initial state of cycling, respectively.  $R_{\text{EOL}}$  is the internal resistance at the end of life (EOL).

The discharge voltage descends faster and the discharge time becomes shorter with aging.<sup>150</sup> In addition to the different pathways both cycle aging and calendar aging, uneven degradation phenomena were observed.<sup>151</sup> The basic step is the conduct of test matrices for aging correlation considering calendar aging mode, cycling aging mode, and mixed aging modes.<sup>152</sup>

With the real-time measurable data, the estimation of the capacity loss and resistance increase can be performed by algebraic expressions of the model in BMS.<sup>153,154</sup> For example, by extracting curve features from the data profile, differential voltage analysis (DVA),<sup>155</sup> incremental capacity analysis (ICA)<sup>156</sup> and differential thermal voltammetry (DTV)<sup>157</sup> can determine the loss of lithium inventory (LLI) and loss of active material (LLA) to compare the lithiation and delithiation capacity for fresh and aged electrodes or cells.<sup>158</sup> The voltage–capacity model-based features of interest extracting optimized the IC fitting accuracy, robustness to aging and the computing cost, allowing real-time applications.<sup>159</sup> A universal approach named the level evaluation analysis is proposed for calculating differentiations in data to derive different types of differential curves (ICA/DVA/DTV).<sup>160</sup> Due to measurement noise, by cross-validation, the robust cubic smoothing spline method on producing IC curves is superior over typical filters that require tuning on window size usually by trial & error.<sup>161</sup> These methods, which extract features to obtain health indicators for

state estimation, have a prediction error of basically less than 5% for health prediction at cell level.

Compared to the SOC, it tends to assign a higher influence of the temperature variations on the capacity loss.<sup>162</sup> To estimate the effect of the current rate on battery aging, maintain a constant room temperature using climatic chambers is still controversial.<sup>163</sup> To link capacity rates to electrode properties, a semiempirical model is used for electrodes fabricated from several materials at various thicknesses.<sup>164</sup> Except for constant current conditions, dynamic profiles can be taken towards the online implementation of the model.<sup>165</sup> SOH prediction still requires various technical support, such as BMS, electrical, electronics, telecommunications, microcontroller technology, *etc.*

#### 4.3 Cyber management

The novel BMS framework seeks to understand the underlying mechanism of CPSs as well as make predictions concerning their state trajectories based on the discovered models.

**4.3.1 Model-driven engineering (MDE).** MDE is a kind of software approach based on three primary activities *i.e.* modelling, model transformation and verification. It incorporates the features of reusability and portability. Such sophisticated features are highly supportive and aligned with the implementation requirements of cloud computing. Consequently, MDE is considered an effective and attractive development approach for cloud computing.

To fulfil different tasks for state estimation and different management strategies, these data are converted to hierarchical structures by a certain methodology which refers to transfer protocols and the proper data processing methods, such as data cleaning, screening, fusion, feature extraction, and clustering, achieving hierarchical computing and control methods.<sup>22</sup> Based on sensing data from the vehicles, a serial of desired models can be established and trained, guiding battery design and optimization process.

Intelligent algorithms and communication technologies are driving the products manufacturing industry toward the big data era. With the physical reproduction process of the cloud data model, the systematic guidance of optimization iteration for the product can be achieved in two different ways. One is to guide the design rules for higher performance, safer, and more environmentally friendly materials. The other is that the conventional product design process is limited to the individual's professional knowledge, while researchers can optimize the processing technology of products by taking advantage of the product usage data collected on the cloud.

**4.3.2 Diagnoses and prognostics health management (PHM).** Progress on the diagnosis of battery degradation has had a substantial effect on the development of EVs. The design of large and complex battery systems require an improved understanding of batteries during operation to diagnose problems and predict performance in real-time. Similarly, the ability to take an unknown cell, and diagnose how it has degraded based upon an understanding of the fundamental degradation mechanisms have been researched for years. However, when



encountering the issues of capacity fade, thermal influence, and energy density changing, most often these models neglect the impact of degradation and are not able to aid in understanding the interactions between components. Chu *et al.* performed real-time diagnostics of LiBs without contact or cell teardown and extracted material properties from external measurements of voltage and temperature.<sup>166</sup> Anseán *et al.* presented a mechanistic investigation that generates a complete degradation mapping coupled with aging features to attain accurate diagnosis and prognosis.<sup>167</sup>

Internal failure including loss of electrode materials, structure deformation and dendrite growth usually incubates from atomic/molecular level and progressively aggravates along with lithiation. It is reported that the variations of voltage and resistance are ahead of the gas release when battery safety declined more sharply.<sup>168</sup> It is suggested that ICA and impedance estimation can be used to detect overcharging cycling online.<sup>169</sup> Excessive heat generation and transfer are easy to melt the separator and lead to cell failure.<sup>170</sup> To identify battery faults, a method based on the empirical mode decomposition and sample entropy is proposed under various operating conditions.<sup>171</sup>

Many LiBs is bound to degrade, eventually leading to severe disposal problem that may pose detrimental impacts on environment and energy conservation. The PHM method is urgently demanding for batteries.<sup>172</sup> To meet energy and cost targets, improvements of PHM through the whole battery value recycling are needed. As shown in Fig. 7, CHAIN is presented to ensure the security and stability of battery full-lifespan, which is an effective tool to optimize battery performances and develop next-generation of energy storages by bringing the virtual thoughts into reality before fabrication.

PHM is a monitoring and predicting system, which can detect battery failure and predict RUL in time employing model-based, data-driven, and hybrid prognostics. The core of PHM is the accurate prediction and reliable analysis of the target batteries. Model-based prognostics demands a balance between the accuracy of valuation results and the complexity of electrochemical mechanisms which require to be updated regularly by incorporating historical data and real-time operation data, while the data-driven approach can be combined with historical database parameter corrections which are more universal, yet more dependent on data accuracy and the calculation speed. The cloud servers of CHAIN process a variety of estimation methods. Therefore, users can choose one or more of them based on computational accuracy requirements and calculation conditions to obtain the desired results. Repurposing degraded LiBs in second use applications holds the potential to reduce first-cost impediments of EVs.<sup>173</sup> Mathews *et al.* used a semi-empirical data-based model of NMC degradation for EV manufacturers to reach break-even and profitability for second-life battery costs that are <60% of the new battery.<sup>174</sup> It has been discovered that the channel choice of capacity allocation and battery recycling is determined by the battery prices of the upstream EV manufacturer and the external supplier.<sup>175</sup>

## 5 Intelligent analysis by machine learning

The 'safety envelope' of temperature and current of the battery system delineates the boundaries of loading conditions of EVs. Reliable operation requires continuous monitoring of sensors and analytical decisions of the BMS. The issue is how to extract the critical parameters leading to battery aging and failure from the growing cumulative data. Due to the complexity of massive

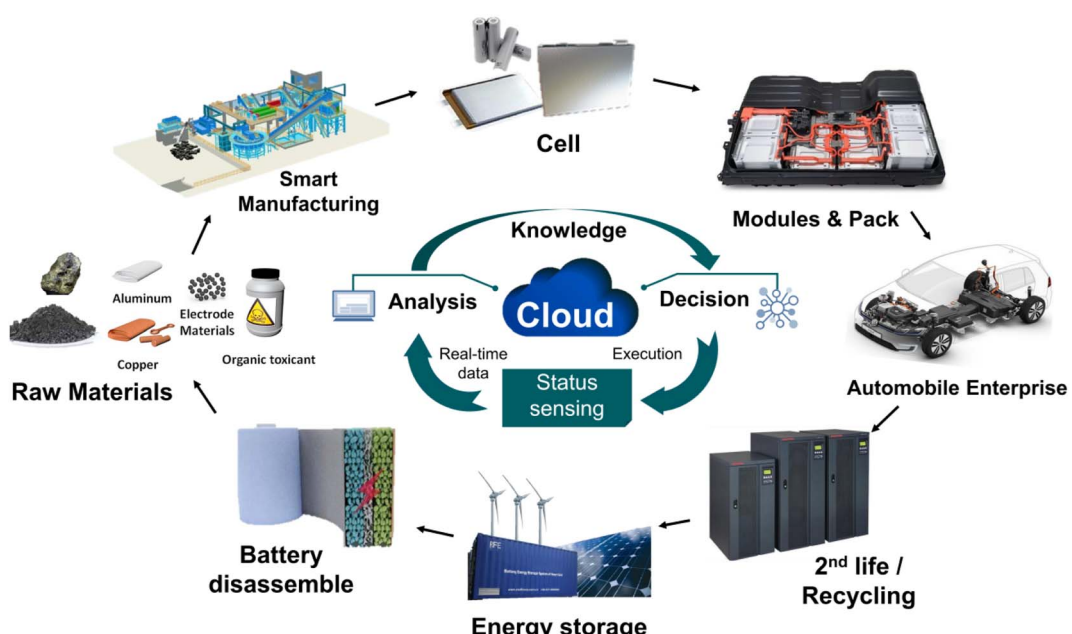


Fig. 7 The prognostics and health management of battery.<sup>22</sup>



data process and analysis, the computer-aided decision-making by ML and the intelligent methodology is of crucial importance when considering the construction of digital clouded BMS. For data extraction and collection, ML algorithms are numerous and increasing rapidly every year. Briefly, ML algorithms can be divided into supervised, unsupervised, semi-supervised and reinforced according to the learning mode. It can also be categorized into classification, regression and clustering based on the learning task. There is no fixed classification criteria, that is, some newer algorithms have more than two characteristics at the same time. This article reviews the ML-dependent algorithms and their characteristics involved in existing BMS literature and listed in Fig. 8, which is not intended to enumerate and classify all machine learning algorithms here. The semi-supervised and supervised learning cover the most state estimation and life prediction applications, as well as attempts at increasing popularity of reinforcement learning and ensemble learning algorithms in recent years.

The promoted classifications of data analysis method can be divided into the unsupervised learning, supervised learning, reinforcement learning and ensemble learning.<sup>176</sup> The ML investigations on energy storage and conversion materials have rapidly increased that has been widely promoted on LiBs owing to the innovation classification or characteristic extraction. In recent years, mathematical models have attracted attention combined with data-driven techniques. These models can make predictions without prior knowledge of the system, and have high accuracy with low computational cost. Currently, the data-driven methodologies are generally originated from

mathematical statistics. Although some methods are outstanding for dealing with the issue of batteries, hardly considerations about the physical principles are adopted for enhancing the algorithms. Therefore, it is worthy to associate the physical model with the data-driven method as the classical researches could benefit the algorithms as the extremely crucial prior technique.<sup>177</sup> Coupling the neural networks with physical principles are presented as the potential research direction.

Due to flexibility and nonlinear matching ability, ML methods are among the most popular data-driven techniques for both health estimation and prediction.<sup>30</sup> Data-driven mathematical models are becoming one of the most prominent approaches to battery health estimation and prediction for real applications as they do not involve complex physical models. There is a strong linear relation between knee-onset, knee-point and end-of-life capacity evolution, that can be predicted by ML techniques.<sup>179</sup> Peter *et al.*<sup>180</sup> proposed a charging optimization approach based on ML. The cycle life of LiBs was maximized by the optimization of parameter space with a specified charging step and duration. Specific, the experimental data of the first few cycles were applied to predict the final cycle life which reduced the time consumption per experiment. Subsequently, the Bayesian optimization algorithm was adopted to detect the parameter space of charging protocols which simplified the experimental procedures. Chen *et al.*<sup>181</sup> focused on materials development where ML has been successfully applied, and reviewed the fundamental procedures to promote further developments in the field of energy storage and conversion.

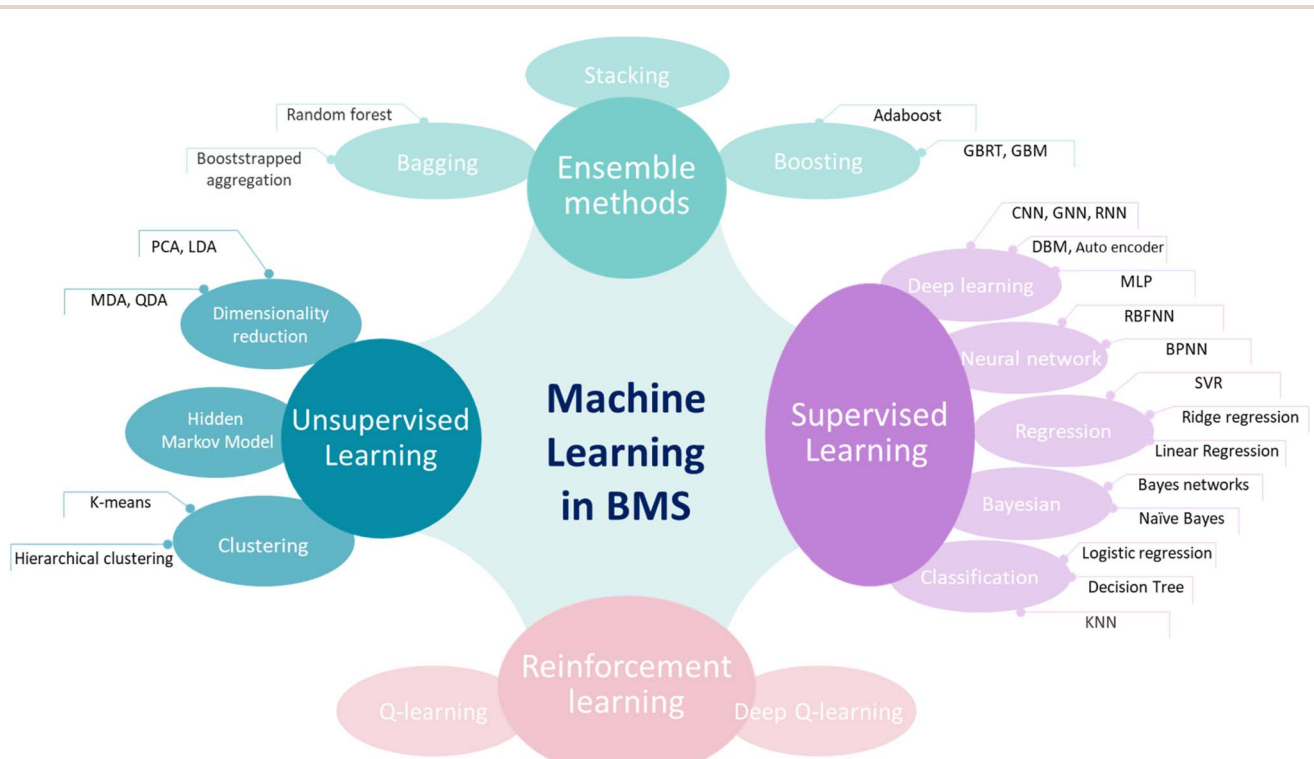


Fig. 8 The characteristics of machine learning-dependent algorithms involved in BMS applications.<sup>178</sup>



## 5.1 Unsupervised learning

Unsupervised learning is essentially a statistical device that uncovers underlying structures in unlabeled data. The mainstream unsupervised learning methods are clustering and dimensionality reduction. As one of the important subjects of ML, clustering-based classification concentrates on the database. The normal clustering method adopted for construction includes *K*-means clustering, *K*-medoids clustering and Clarans clustering, and all method could show satisfactory performance.<sup>182</sup> The research on combining data mining techniques with machine learning methods for fault diagnosis and safety management of complex power systems is also promising. By analysing anomalies hidden under external measurements and calculating the failure frequency of each battery pack, the clustering algorithm can identify the fault type and locate the faulty unit in time.<sup>183</sup> You *et al.* proposed a data-driven framework by applying the *K*-means clustering algorithm to trace the SOH of batteries that are cycled dynamically according to various driving patterns.<sup>184</sup> The driving cycles are velocity/power-time curves and always used for vehicle testing to determine the emission or energy consumption. Owing to the representation of the local traffic conditions, the development of driving cycles is based on the kinematic fragments sampling from the local vehicles. And clustering is adopted to classify the samples fundamental on the characteristics of each kinematic fragment. Some urban cities have constructed the local driving cycles based on the clustering, including China (Beijing,<sup>185</sup> Xi'an,<sup>186</sup> Shenyang<sup>187</sup>) and India.

## 5.2 Supervised learning

During the training process of supervised learning algorithms, a pattern can be established from the training dataset, such as a functional relationship or a learning model, and new instances can be inferred based on this pattern. The algorithm requires specific inputs/outputs, and first needs to decide which data to use as an example. The main algorithms include classification, regression, Bayesian method, neural networks and deep learning.

The representative use is classification, to allocate labels for the samples in the database based on the characteristics. Different from clustering, the supporting vector machine (SVM) is one of the supervised learnings based on a generalized linear classifier.<sup>188</sup> The samples are gathered in a high dimensional space and classified if projected into lower dimensional space with a hyperplane. Therefore, the pivotal factor of SVM is to determine the maximum-margin hyperplane according to the learning from the database.<sup>189</sup> Currently, SVM can be achieved by researching the kernel method, and the robustness and stabilities due to the regularization to avoid the structural risk.<sup>190</sup> The representative application for SVM is to classify the batteries and search for the battery with worse consistency.<sup>191</sup> The batteries in the same packs may be inconsistent due to the distribution of temperature and current, resulting in the imprecise estimation of battery SOC. To enhance the accuracy, tracking the batteries with worse consistency in the pack is an effective method. However, the effect of polarization makes it

hard to identify the targeted battery. Therefore, the SVM is taken advantages of for outstanding classification of batteries. Some researches indicate that SVM and the improvements have satisfactory performance and might be widely promoted for the future clouded BMS.

Other applications have been researched. Feng *et al.* introduced the method for SOH and a maximum error of 2% could be achieved.<sup>182</sup> Methods including logistic regression and relevance vector machine<sup>192</sup> are also used for application on LiBs. The main courses are concentrating on state estimation. For instance, the SOH represents the current capacity of the batteries, influencing the driving range and safety. And the ML methods are adopted to achieve high precision of SOH estimation and prediction.<sup>193</sup>

Bayesian algorithm is based on probability theory and statistics knowledge to complete classification, which requires the efficient sample data that independent of each other.<sup>194</sup> It has the characteristics of high classification accuracy and fast speed. Hierarchical Bayesian models (HBMs) provide rapid prediction of LFP performance under high-rate charging.<sup>195</sup> Attia *et al.* predicted the final cycle life with the help of Bayesian optimization algorithm and cycle data from previous cycles, provided future charging parameters and optimized charging strategies.<sup>196</sup>

**5.2.1 Neural network.** Neural networks are an algorithm used for supervised learning, which can automatically learn useful knowledge from the data without an accurate mathematical model. Various scenarios are found as the fast promotion of neural network (NN), and there have been enough variants that could be used in clouded BMS.

Back propagation (BP) is the basic NN that can be used for distributed parallel information processing. The essential issue for BP is gradient descending, and the training of BP relies on the method for back propagation of error. Several hidden layers are composed and each layer is with a weight that represents the relationship between inlets and outlet. BP networks are widely promoted in system identification, and the main application in batteries is SOC estimation. The SOC estimation is summarized as a maximum posterior estimation, where the state is associated with the previous ones. The BP networks can describe the connection between the input current and the output SOC. The main idea for achievement is to supply enough database to train the BP network for tackling the probability conditions. Although the algorithms can achieve a satisfactory result based on the training database, the generalization might be imprecise if the input is out of the training database. Other applications including the identification of models are under-researched.<sup>197,198</sup>

Elman neural networks are representative dynamic recurrent NN, which emphasizes the ability for tackling the time-varying system. The specialization of Elman neural networks is that an extra layer, namely the bearing layer, is applied to the original NNs and the lagging effect can be achieved. The bearing layer has the ability for memorizing the information of former layers, makes it possible to address the sensitivity between the continuous training database. While similarly with BP networks, the Elman neural networks still rely on the gradient



descending method, indicating that the methodology may have difficulty for convergence. Though the popular application for SOH estimation still makes it to be a powerful tool, and the stability and robustness are rather better than the previous methods. Some researchers have been carried out to utilize the Elman neural networks for state estimation, including SOH,<sup>199,200</sup> and the result analysis illustrates a better performance. The main advantage of the NN model is that it is suitable for all types of batteries, but it requires sufficient training data samples and time-consuming training period.

**5.2.2 Deep learning.** Deep learning is an innovative field that originated from neural network and has attracted much attentions to deal with the issue of image identification and data mining. At present, deep learning algorithms are widely used in many fields, for example, electric load forecasting, traffic speed prediction, and fault diagnosis systems, which makes it possible for applying in batteries. Compared to the NN algorithm, the deep learning algorithm could effectively simulate highly nonlinear mapping between the input and output. Therefore, it can accurately model the battery under a multi-variable environment and dynamic conditions.

Recurrent neural network (RNN)<sup>201</sup> has been extensively utilized to diagnose and prognosis LiBs, as it has demonstrated superior performance. It is also applied to the recognition of driving patterns and applied to energy management optimization.<sup>202</sup> A gated recurrent unit recurrent neural network (GRU-RNN) based momentum optimized SOC estimation algorithm is investigated to promote the SOC convergence speed and prevent overfitting.<sup>203</sup> The framework of a multi-scale model that couples a deep NN with a partial differential equation solver can provide an understanding of the relationship between the pore-scale electrode structure reaction and device-scale electrochemical reaction uniformity.<sup>204</sup> For the first time, a feed-forward artificial neural network (ANN) has been used to estimate the SOC of calendar-aged lithium-ion pouch cells.<sup>205</sup>

For instance, a variant long-short-term memory (LSTM) NN prognostic framework shared by multiple batteries is well-trained separately for the prediction of SOH and remaining useful life (RUL).<sup>206</sup> A deep learning-based capacity estimation method that incorporates the concepts of transfer learning and ensemble learning avoiding the costly and time-consuming data production process.<sup>207</sup>

Due to the original RNNs has trouble convergence relying on the gradient descending method, RNNs may encounter the trouble of vanishing gradient or over-large gradient according to the disability for long-term memory, failing networks training. As improvements, some memory units are introduced to achieve the memory between continuous layers with some controlling gates, resulting in the enhanced ability for long-term memory, leading to the better performance of dealing with the sequent database. Due to the degradation of batteries is strongly associated with the historical path, the batteries state always has the potential relations between the continuous samples. The normal neural networks do not perform well for taking the advantages of sequence in time, and some essential information could be obliged. Researches introduced the LSTM to utilize the information hidden in the database as much, and

a satisfactory performance could be achieved within sufficient training.<sup>208</sup> Bian *et al.* introduced a SOC estimation based on LSTM and the adaptability for different batteries are valid.<sup>209</sup> Hong *et al.* proposed a joint-prediction strategy using LSTM and multiple linear regression algorithms and takes into account weather and drivers' driving behaviours during real vehicular operating has excellent practical application effects.<sup>210</sup> LSTM recurrent neural network performs accurate synchronous multi-parameter prediction for battery systems.<sup>211</sup>

Distinguished from the normal NN, DNNs have a better performance for simulating the nonlinear system and could save more sources. DNNs could be considered as the improvements for NNs, and more hidden layers (generally more than 2 layers) are utilized to imitate the brain way of thinking. DNNs are popular to deal with the RUL issues, and more application scenarios are under research.<sup>212</sup> Ren *et al.*<sup>213</sup> proposed an integrated DNN to predict RUL and the method is validated based on the database of NASA. Other applications can be taken into consideration, such as the diagnosis of LiBs. Cadini *et al.*<sup>7</sup> introduced data-driven particle filters to achieve lifetime prognosis and diagnosis, and Khaleghi *et al.*<sup>214</sup> introduced a real-time health diagnosis method based on data-driven.

### 5.3 Reinforcement learning

The learning-based BMS benefits from the development of machine learning. The supervised learning treats the optimal control result as the label data and employs the neural network to fit the mapping relationship between the state and the action. While the reinforcement learning (RL) takes the iterative trial-and-error method by the data conversion between the environment and the agent to search for the optimal control strategy.<sup>215</sup> It reflects a mapping between the random state and the optimal action, which can guarantee adaptability.<sup>216</sup> The network could learn how to take the actions based on the rewards by RL, and then maximize the notion of cumulative rewards to search for the best solution.<sup>217</sup> Due to the model-free and self-learning performance, RL has been widely promoted for BMS, especially energy management. Other issues including SOC estimation could be researched based on RL.<sup>218</sup>

The issue of energy management can be abstract as the strategy for batteries to release more energy for driving, and it could be similar to the problem of optimization. The issue is crucial for future intelligent driving coupled with connected vehicles, and various researches have been carried out. Zhou *et al.*<sup>219</sup> introduced an energy management method based on RL, and the simulation results indicate that at least 7.8% of energy could be saved.

Several pieces of research have been carried out and they might extend the method to achieve the improvement for clouded BMS. Tian *et al.*<sup>220</sup> proposed a method coupling LSTM and cubature Kalman filter for SOC estimation, and a maximum error of 4% could be observed. And Kim *et al.*<sup>221</sup> introduced a method based on deep Bayesian harmony search for model identification. Song *et al.*<sup>20</sup> proposed a method coupling SVM and unscented Kalman filter to co-estimate SOC and SOH.



## 6 Hybrid applications based on fusion schemes

In EVs, onboard BMS is responsible for monitoring the battery's basic conditions such as voltage, current and temperature. Empirical methods can be easily used onboard. However, the obvious disadvantage is their dependence on empirical knowledge, which is unlikely to encompass all the complex conditions and some of the pre-unknown working conditions of batteries.

The control-oriented applications on vehicles are necessary by means of computationally efficient models. Undoubtedly, it appears very important to improve the calculation efficiency for real-time applications. The integrated 5-state model is computationally efficient for vehicle applications and provides estimates of the critical battery states. From a software perspective, onboard diagnosis using lookup tables with selected features of interest of the incremental capacity curves can be implemented before its deployment.<sup>222</sup> When the vehicle is running or charging, the BMS will regulate the temperature of the batteries, so it is most important to be aware of high battery temperatures when the vehicle is parked.<sup>223</sup> The charging pattern transits from constant DC to AC and adopts optimization and adaptive estimation algorithms, which have improved charging performances and provided valuable experiences for further study.<sup>224</sup>

Onboard state estimation algorithms that should be able to be implemented onboard real buses, using commercial, inexpensive measuring hardware are favourable for obtaining valuable feedback to recalibrate. Research has shown the viability of acceptance of deep learning-based prognostics in future battery management systems.<sup>225</sup> Furthermore, the SOX needs to be estimated by specific algorithms as it cannot be directly measured during battery operation.<sup>226</sup> Therefore, in cases in which the model has trained onboard, the accuracy and real-time of the algorithm may also affect the performance of the model.<sup>227</sup> However, it is recommended that, when the LiBs are used on vehicles, yearly recalibration is made, to keep the algorithm in touch with the actual state of life.

It is noted that the higher efficiency methodology is more suitable for onboard estimation devices that require computationally efficient estimation techniques. Owing to the complexity of onboard implementation, low computation algorithms like Kalman filter are capable of solid surface concentration and phase potential estimation, if possible, would provide a more elegant onboard solution. For limited BMS memory space, it is presented the frequency division model of the battery pack to reconstruct the voltage distortion recorded with the lower recording frequency.<sup>228</sup> In addition, what is required is driver behaviour analysis, and personal energy analysis models to provide users with private driving forecasts and recommendations. For example, the best charging method, the remaining battery mileage reminder, battery life prediction.

The existing cloud management platform mostly has a three-tier platform structure of the enterprise, local and national. First, data acquisition and fusion for state and GPS are completed on the vehicle, which is visible to the enterprises.

Then, these data will be transmitted to the national platform for specific management. The data includes but not limited to drive motor, extreme value, alarm, vehicle position, engine, temperature and voltage of cells. The analysis of data characteristics related to battery mechanism is necessary considering the best suitable method of data mining. Herein, several representative methodologies and their preferable applications are presented. If the automotive industry has the application of cloud management technology, then with the combination of big data and internet of things technology, driverless cars can enter people's lives. Sharing and management of traffic data provide solutions for smart transportation soon. Achieving driverless or automatic driving is just around the corner.

The imminent coupling of the transport sector with the electricity sector and the possibilities of grid integrated energy storages are creating new potentials and challenges.<sup>229</sup>

The manufacturing industry mentioned above, the earliest application of digital hygiene technology: using industrial big data to improve the manufacturing level, including product fault diagnosis and prediction, analysis of process flow, improvement of production process, optimization of production process energy consumption, industrial supply chain analysis and optimization, production planning and scheduling.

Several studies focus on the fundamental risks and issues associated with battery safety and reliability. Industry challenges with fielding safe and reliable batteries are increasing as new cell designs are introduced into advanced energy storage applications requiring higher specific energies, fast charging, and lower-cost alternatives. Likewise, improvements in cell and battery safety design without compromising performance continues to be a major focus for researchers, manufacturers, and users across all sectors of the energy storage marketplace. A better understanding of battery failure mechanisms will further enable regulatory agency approval and public acceptance of early deployment of advanced battery energy storage systems for high-reliability applications.

The authors believe that digital twins technology have the potential for module and system modelling and EV applications. With digital twins, building complex and accurate battery system models in the cloud can be implemented, which is briefly called cloud modelling. Since the cloud provides enough memory and computational effort, there is no need to consider the limitations of model complexity. Cloud modelling may implement the whole life cycle simulation and modification of the battery, helping the BMS to manage and control the battery better.

## 7 Conclusions

Interactional management is vigorously developing in EV fields as a fire-new and highly effective framework for battery monitor and management. CHAIN presented in Section 2 is the typical one of the many possible manifestations. Inspired by the multiple scale framework, a comprehensive review of the development of battery management is introduced and discussed from different spatial dimensions (material to the



system), dynamic dimensions (microsecond to year), and time dimensions (past to future). The review comprises four aspects:

(1) For high energy density, excellent performance and safety, the comprehensive research of LiBs at multi-scale is essential from the electrode to pack. This paper focuses more on the recent developments in this field.

(2) Modelling and state estimation is given considering multiple domains include battery electrical, thermal, aging, and further coupled domains. The whole process of model development is traced based on the modelling philosophy, utility, and application.

(3) Intelligence is the most distinctive features of next-generation management. This review highlighted the attempts of AI methods on battery data analysis. Intelligent methods offer novel tools to tackle mass data computing on the cloud. The innovative theory for data mining that might be promoted in the future is still introduced for providing the probable advanced research direction.

(4) This paper presented the cutting-edge battery management technologies in achieving satisfactory safety and long service life for EV applications. With the help of data computing, the cloud-based training and serving to localized devices are an optimal combination for accuracy and time-efficient. The need to develop reliable onboard applications enabling interactional management is highlighted as well as data-driven technologies for battery health diagnostics and prognostics. Scientific literature covering the above topics is analyzed, and each approach is discussed in view of its advantages and pitfalls.

In summary, considerably advanced attempts exist in the literature including but not limited to onboard dynamic condition for computationally tractable models in a wide variety of tasks and applications. Although many valuable applications can be performed based on intelligent management, there are still some engineering and scientific challenges faced for current technologies, devices during generalization and application. The main challenges are as follows:

(1) Data: all walks of life including finance, automotive, catering, telecommunications, energy, entertainment, *etc.*, have integrated the traces of big data. Data is an essential precondition for the timely and accurate judgement of the battery. The measurable physical quantities for batteries are limited to voltage, current, and temperature. Firstly, the novel sensing technology will generate higher dimensions data and bring tremendous innovation for battery modelling, state estimation, and management strategies. Secondly, the communication system, method, apparatus and digital interface for data transmission need an upgrade to meet timeliness and correctness. Finally, security issues such as authentication, data segregation, and encryption are considered as the top concerns in cloud computing. Information security and privacy also shall be taken into consideration.

(2) Algorithm: with the proliferation of massive and diverse scientific data, the ability of machines to intelligently process and use data needs to be improved. The new generation of technologies such as ML and AI will play an increasingly important role. Determining how to generate and use converged

cyber-physical data to better serve battery lifecycle, to drive cell/pack design, manufacturing, and service to be more efficient, smart, and sustainable is emphasized and investigated based on our pre-existing study on big data in BMS. Data processing technology barriers must be reduced to make analytical tools more accessible and to improve data and visualization literacy, especially the generality of the algorithm.

(3) Application: the development opportunities and challenges of cloud-based technology based on digital twins coexist. The current advanced AI algorithms, such as filters, observers and ML, are still difficult to apply online due to the limited computing capability of the vehicle-mounted controller. With the increasing complicating algorithms and battery models designed for lifetime, safety, and performance, the management system needs a more detailed and clear division of tasks for interactional distributed management. Therefore, an efficient and intelligent computing framework will bring great changes to next-generation battery management technology.

## Author contributions

Rong He: conceptualization, writing – original draft, writing – review & editing, visualization, funding acquisition. Wenlong Xie: writing – review. Billy Wu: writing – review. Nigel P. Brandon: writing – review. Xinhua Liu: conceptualization. Xinghu Li: funding acquisition. Shichun Yang: supervision, project administration, funding acquisition.

## Conflicts of interest

There are no conflicts to declare.

## Acknowledgements

This work was supported by the National Key Research and Development Program of China (2021YFB2501500); the National Natural Science Foundation of China (No. U1864213); and the China Scholarship Council (File No. 202006020203).

## References

- 1 J. Wang, H. Li, H. Lu, H. Yang and C. Wang, *J. Cleaner Prod.*, 2020, **247**, 119095.
- 2 H. Dai, B. Jiang, X. Hu, X. Lin, X. Wei and M. Pecht, *Renewable Sustainable Energy Rev.*, 2021, **138**, 110480.
- 3 Y. Wang, Z. Sun and Z. Chen, *Appl. Energy*, 2019, **254**, 419–433.
- 4 F. Basic, M. Gaertner and C. Steger, *Int. J. Radio Freq. Identif.*, 2022, **7281**, 1–12.
- 5 S. chun Yang, Y. Hua, D. Qiao, Y. bo Lian, Y. wei Pan and Y. ling He, *Electrochim. Acta*, 2019, **326**, 134928.
- 6 P. Li, J. Liu, Z. Deng, Y. Yang, X. Lin, J. Couture and X. Hu, *Energy*, 2022, **243**, 122772.
- 7 F. Cadini, C. Sbarufatti, F. Cancelliere and M. Giglio, *Appl. Energy*, 2019, **235**, 661–672.
- 8 W. Zhu, *Int. J. Energy Res.*, 2022, 1–14.
- 9 J. Li and Z.-F. Ma, *Chem*, 2019, **5**, 3–6.



10 M. Adaikkappan and N. Sathiyamoorthy, *Int. J. Energy Res.*, 2022, **46**, 2141–2165.

11 W. Zhang, L. L. Wang, L. L. Wang, C. Liao and Y. Zhang, *IEEE Trans. Ind. Electron.*, 2022, **69**, 3677–3688.

12 J. S. Qiu, Y. C. Fan, S. L. Wang, X. Yang, J. L. Qiao and D. L. Liu, *Int. J. Energy Res.*, 2022, **46**, 13931–13946.

13 J. Wu, C. Fang, Z. Jin, L. Zhang and J. Xing, *J. Energy Storage*, 2022, **50**, 104666.

14 Y. Wang, R. Xu, C. Zhou, X. Kang and Z. Chen, *J. Manuf. Syst.*, 2022, **62**, 124–134.

15 B. Wu, W. D. Widanage, S. Yang and X. Liu, *Energy AI*, 2020, **1**, 100016.

16 C. Xu, L. Li, Y. Xu, X. Han and Y. Zheng, *eTransportation*, 2022, **12**, 100172.

17 F. Tao, J. Cheng, Q. Qi, M. Zhang, H. Zhang and F. Sui, *Int. J. Adv. Des. Manuf. Technol.*, 2018, **94**, 3563–3576.

18 D. Qiao, X. Wei, W. Fan, B. Jiang, X. Lai, Y. Zheng, X. Tang and H. Dai, *Appl. Energy*, 2022, **317**, 119168.

19 Y. Yuan, X. Tang, W. Zhou, W. Pan, X. Li, H. T. Zhang, H. Ding and J. Goncalves, *Nat. Commun.*, 2019, **10**, 1–9.

20 Y. Song, D. Liu, H. Liao and Y. Peng, *Appl. Energy*, 2020, **261**, 114408.

21 T. Sun, S. Wang, S. Jiang, B. Xu, X. Han, X. Lai and Y. Zheng, *Energy*, 2022, **239**, 122185.

22 S. Yang, R. He, Z. Zhang, Y. Cao, X. Gao and X. Liu, *Matter*, 2020, **3**, 27–41.

23 S. Yang, Z. Zhang, R. Cao, M. Wang, H. Cheng, L. Zhang, Y. Jiang, Y. Li, B. Chen, H. Ling, Y. Lian, B. Wu and X. Liu, *Energy AI*, 2021, **5**, 100088.

24 S. Li, H. He and J. Li, *Appl. Energy*, 2019, **242**, 1259–1273.

25 K. Liu, Z. Wei, C. Zhang, Y. Shang, R. Teodorescu and Q. L. Han, *IEEE/CAA J. Autom. Sin.*, 2022, **9**(7), 1139–1165.

26 C. H. Lee and C. H. Wu, *Proc. – 12th Int. Conf. Inf. Technol. New Gener. ITNG*, 2015, vol. 2015, pp. 626–631.

27 S. Li, J. Li, H. He and H. Wang, *Energy Procedia*, 2019, **159**, 168–173.

28 Z. Zhao, L. Zhang, M. Yang, J. Chai and S. Li, *J. Cleaner Prod.*, 2020, **254**, 120039.

29 S. Hu, P. Chen, F. Xin and C. Xie, *Transp. Res. D: Transp. Environ.*, 2019, **77**, 164–177.

30 Y. Li, K. Liu, A. M. Foley, A. Zülke, M. Berecibar, E. Nanini-Maury, J. Van Mierlo and H. E. Hoster, *Renewable Sustainable Energy Rev.*, 2019, **113**, 109254.

31 M. Behrisch, D. Streeb, F. Stoffel, D. Seebacher, B. Matejek, S. H. Weber, S. Mittelstaedt, H. Pfister and D. Keim, *IEEE Trans. Vis. Comput. Graph.*, 2018, **25**, 3011–3031.

32 S. Huang, X. Wu, G. M. Cavalheiro, X. Du, B. Liu, Z. Du and G. Zhang, *J. Electrochem. Soc.*, 2019, **166**, A3254–A3259.

33 M. Spielbauer, P. Berg, M. Ringat, O. Bohlen and A. Jossen, *J. Energy Storage*, 2019, **26**, 101039.

34 G. Seo, J. Ha, M. Kim, J. Park, J. Lee, E. Park, S. Bong, K. Lee, S. J. Kwon, S. pil Moon, J. Choi and J. Lee, *J. Energy Chem.*, 2022, **67**, 663–671.

35 L. H. J. Raijmakers, D. L. Danilov, R. A. Eichel and P. H. L. Notten, *Appl. Energy*, 2019, **240**, 918–945.

36 Y. Zhao, P. Stein, Y. Bai, M. Al-Siraj, Y. Yang and B. X. Xu, *J. Power Sources*, 2019, **413**, 259–283.

37 L. Wang, X. Duan, B. Liu, Q. M. Li, S. Yin and J. Xu, *J. Power Sources*, 2020, **448**, 227468.

38 X. Gao, W. Lu and J. Xu, *J. Power Sources*, 2020, **449**, 227501.

39 B. Prifling, D. Westhoff, D. Schmidt, H. Markötter, I. Manke, V. Knoblauch and V. Schmidt, *Comput. Mater. Sci.*, 2019, **169**, 109083.

40 J. Le Houx and D. Kramer, *Energy Rep.*, 2020, **6**, 1–9.

41 X. Meng, Y. Xu, H. Cao, X. Lin, P. Ning, Y. Zhang, Y. G. Garcia and Z. Sun, *Green Energy Environ.*, 2020, **5**, 22–36.

42 H. Li, M. Xu, C. Gao, W. Zhang, Z. Zhang, Y. Lai and L. Jiao, *Energy Storage Mater.*, 2020, **26**, 325–333.

43 Y. Kuang, C. Chen, D. Kirsch and L. Hu, *Adv. Energy Mater.*, 2019, **9**, 1–19.

44 S. H. Park, P. J. King, R. Tian, C. S. Boland, J. Coelho, C. J. Zhang, P. McBean, N. McEvoy, M. P. Kremer, D. Daly, J. N. Coleman and V. Nicolosi, *Nat. Energy*, 2019, **4**(7), 560–567.

45 K. Yoo, P. Dutta and S. Banerjee, *ASME Int. Mech. Eng. Congr. Expo. Proc.*, 2015, **6A**, 2015, pp. 301–310.

46 D. Grazioli, O. Verners, V. Zadin, D. Brandell and A. Simone, *Electrochim. Acta*, 2019, **296**, 1122–1141.

47 C. M. Costa, Y. H. Lee, J. H. Kim, S. Y. Lee and S. Lanceros-Méndez, *Energy Storage Mater.*, 2019, **22**, 346–375.

48 A. Sarkar, P. Shrotriya and A. Chandra, *J. Power Sources*, 2019, **435**, 226756.

49 H. Xu, M. Zhu, J. Marcicki and X. G. Yang, *J. Power Sources*, 2017, **345**, 137–145.

50 A. D. Sendek, Q. Yang, E. D. Cubuk, K. A. N. Duerloo, Y. Cui and E. J. Reed, *Energy Environ. Sci.*, 2017, **10**, 306–320.

51 I. D. Campbell, K. Gopalakrishnan, M. Marinescu, M. Torchio, G. J. Offer and D. Raimondo, *J. Energy Storage*, 2019, **22**, 228–238.

52 W. B. Hawley and J. Li, *J. Energy Storage*, 2019, **25**, 100862.

53 D. Miranda, A. Gören, C. M. Costa, M. M. Silva, A. M. Almeida and S. Lanceros-Méndez, *Energy*, 2019, **172**, 68–78.

54 K. He, Z. Y. Zhang and F. S. Zhang, *J. Hazard. Mater.*, 2020, **386**, 121633.

55 M. K. Shobana, *J. Alloys Compd.*, 2019, **802**, 477–487.

56 H. Zhang and J. Zhang, *eTransportation*, 2021, **7**, 100105.

57 M. Chouchane, A. Rucci, T. Lombardo, A. C. Ngandjong and A. A. Franco, *J. Power Sources*, 2019, **444**, 227285.

58 H. Liu, X. Cheng, Y. Chong, H. Yuan, J. Q. Huang and Q. Zhang, *Particuology*, 2021, **57**, 56–71.

59 C. E. Aimo and P. A. Aguirre, *J. Energy Storage*, 2020, **30**, 101515.

60 F. Duffner, M. Wentker, M. Greenwood and J. Leker, *Renewable Sustainable Energy Rev.*, 2020, **127**, 109872.

61 H. Sun, J. Zhu, D. Baumann, L. Peng, Y. Xu, I. Shakir, Y. Huang and X. Duan, *Nat. Rev. Mater.*, 2019, **4**, 45–60.

62 Y. Pang, Y. Cao, Y. Chu, M. Liu, K. Snyder, D. MacKenzie and C. Cao, *Adv. Funct. Mater.*, 2020, **30**, 1–22.

63 Y. Li, J. Hu, K. Yang, B. Cao, Z. Li, L. Yang and F. Pan, *Mater. Today Energy*, 2019, **14**, 100332.



64 S. Zhu, J. Han, H. Y. An, T. S. Pan, Y. M. Wei, W. L. Song, H. Sen Chen and D. Fang, *J. Power Sources*, 2020, **456**, 227981.

65 M. Yuan and K. Liu, *J. Energy Chem.*, 2020, **43**, 58–70.

66 J. Newman and W. Tiedemann, *AIChE J.*, 1975, **21**, 25–41.

67 E. Hosseinzadeh, J. Marco and P. Jennings, *Appl. Math. Models*, 2018, **61**, 107–123.

68 J. S. Newman and C. W. Tobias, *J. Electrochem. Soc.*, 1962, **109**, 1183.

69 X. Zhang, Y. Gao, B. Guo, C. Zhu, X. Zhou, L. Wang and J. Cao, *Electrochim. Acta*, 2020, **343**, 136070.

70 L. Wang, S. Yin, C. Zhang, Y. Huan and J. Xu, *J. Power Sources*, 2018, **392**, 265–273.

71 C. von Lüders, J. Keil, M. Webersberger, A. Jossen, C. Von Lüders, J. Keil, M. Webersberger and A. Jossen, *J. Power Sources*, 2019, **414**, 41–47.

72 P. Arora, M. Doyle and R. E. White, *J. Electrochem. Soc.*, 1999, **146**, 3543–3553.

73 M. Doyle, T. F. Fuller and J. Newman, *J. Electrochem. Soc.*, 1993, **140**, 1526–1533.

74 M. Lang, M. S. Dewi Darma, L. Mereacre, V. Liebau and H. Ehrenberg, *J. Power Sources*, 2020, **453**, 227915.

75 I. D. Campbell, M. Marzook, M. Marinescu and G. J. Offer, *J. Electrochem. Soc.*, 2019, **166**, A725–A739.

76 F. Ringbeck, C. Rahe, G. Fuchs and D. U. Sauer, *J. Electrochem. Soc.*, 2020, **167**, 090536.

77 B. Shrestha, P. M. Novak, D. A. Wetz and A. F. Matasso, *ECS Trans.*, 2014, **58**(48), 207–222.

78 D. Baker and M. Verbrugge, *J. Electrochem. Soc.*, 2020, **167**(1), 013504.

79 J. Sturm, A. Rheinfeld, I. Zilberman, F. B. Spingler, S. Kosch, F. Frie and A. Jossen, *J. Power Sources*, 2019, **412**, 204–223.

80 S. Yuan, S. Weng, F. Wang, X. Dong, Y. Wang, Z. Wang, C. Shen, J. L. Bao, X. Wang and Y. Xia, *Nano Energy*, 2021, **83**, 105847.

81 Z. Shadike, H. Lee, O. Borodin, X. Cao, X. Fan, X. Wang, R. Lin, S. M. Bak, S. Ghose, K. Xu, C. Wang, J. Liu, J. Xiao, X. Q. Yang and E. Hu, *Nat. Nanotechnol.*, 2021, **16**, 549–554.

82 Y. Zhou, M. Su, X. Yu, Y. Zhang, J. G. Wang, X. Ren, R. Cao, W. Xu, D. R. Baer, Y. Du, O. Borodin, Y. Wang, X. L. Wang, K. Xu, Z. Xu, C. Wang and Z. Zhu, *Nat. Nanotechnol.*, 2020, **15**, 224–230.

83 L. Liu and M. Zhu, *ECS Trans.*, 2014, **61**(27), 33–43.

84 D. Li, H. Li, D. L. Danilov, L. Gao, X. Chen, Z. Zhang, J. Zhou, R. A. Eichel, Y. Yang and P. H. L. Notten, *J. Power Sources*, 2019, **416**, 163–174.

85 B. Horstmann, F. Single and A. Latz, *Curr. Opin. Electrochem.*, 2019, **13**, 61–69.

86 F. Single, A. Latz and B. Horstmann, *ChemSusChem*, 2018, **1950**, 12.

87 S. Das, P. M. Attia, W. C. Chueh and M. Z. Bazant, *J. Electrochem. Soc.*, 2019, **166**, E107–E118.

88 I. Zilberman, S. Ludwig, M. Schiller and A. Jossen, *J. Energy Storage*, 2020, **28**, 101170.

89 X. Liu, W. Ai, M. Naylor Marlow, Y. Patel and B. Wu, *Appl. Energy*, 2019, **248**, 489–499.

90 C. Liu, H. Li, X. Kong and J. Zhao, *Int. J. Heat Mass Transfer*, 2020, **153**, 119590.

91 A. Pozzi, M. Torchio, R. D. Braatz and D. M. Raimondo, *J. Power Sources*, 2020, **461**, 228133.

92 M. F. R. Zwicker, M. Moghadam, W. Zhang and C. V. Nielsen, *J. Adv. Join. Process.*, 2020, **1**, 100017.

93 Y. wei Pan, Y. Hua, S. Zhou, R. He, Y. Zhang, S. Yang, X. Liu, Y. Lian, X. Yan and B. Wu, *J. Power Sources*, 2020, **459**, 228070.

94 J. Chiew, C. S. Chin, W. D. Toh, Z. Gao, J. Jia and C. Z. Zhang, *Appl. Therm. Eng.*, 2019, **147**, 450–463.

95 J. Kleiner, L. Lechermann, L. Komsisyska, G. Elger and C. Endisch, *J. Energy Storage*, 2021, **40**, 102686.

96 S. Gantenbein, M. Weiss and E. Ivers-Tiffée, *J. Power Sources*, 2018, **379**, 317–327.

97 Y. Li, M. Vilathgamuwa, T. Farrell, S. S. Choi, N. T. Tran and J. Teague, *Electrochim. Acta*, 2019, **299**, 451–469.

98 Y. He, R. He, B. Guo, Z. Zhang, S. Yang, X. Liu, X. Zhao, Y. Pan, X. Yan and S. Li, *J. Electrochem. Soc.*, 2020, **167**, 090532.

99 Q. Zhang, N. Cui, Y. Li, B. Duan and C. Zhang, *J. Energy Storage*, 2020, **27**, 100945.

100 J. Yang, Y. Cai and C. C. Mi, *IEEE Trans. Transp. Electrif.*, 2022, **8**, 2070–2079.

101 D. Guo, G. Yang, X. Feng, X. Han, L. Lu and M. Ouyang, *J. Energy Storage*, 2020, **30**, 101404.

102 A. Nasser Eddine, B. Huard, J. D. Gabano, T. Poinot, A. Thomas and S. Martemianov, *IFAC-PapersOnLine*, 2018, **51**, 802–807.

103 A. Calborean, O. Bruj, T. Murariu and C. Morari, *J. Energy Storage*, 2020, **27**, 101143.

104 S. Oswald, D. Pritzl, M. Wetjen and H. A. Gasteiger, *J. Electrochem. Soc.*, 2020, **167**, 100511.

105 Y. Bai, Y. Zhao, W. Liu and B. X. Xu, *J. Power Sources*, 2019, **422**, 92–103.

106 X. Kong, G. L. Plett, M. Scott Trimboli, Z. Zhang, D. Qiao, T. Zhao and Y. Zheng, *J. Energy Storage*, 2020, **27**, 101085.

107 Z. Chu, G. L. Plett, M. S. Trimboli and M. Ouyang, *J. Energy Storage*, 2019, **25**, 100828.

108 Z. Liu, S. Chen, H. Wu, H. Huang and Z. Zhao, *Adv. Theory Simul.*, 2022, **5**, 1–11.

109 H. Pang, L. Mou, L. Guo and F. Zhang, *Electrochim. Acta*, 2019, **307**, 474–487.

110 J. Li, R. G. Landers and J. Park, *J. Power Sources*, 2020, **456**, 227950.

111 Z. Y. Jiang, Z. G. Qu and L. Zhou, *Int. J. Heat Mass Transfer*, 2018, **123**, 500–513.

112 A. Mashayekh, M. Khorasani, J. Estaller, J. Buberger, M. Kuder, R. Eckerle and T. Weyh, *PCIM Eur. Conf. Proc.*, 2022, pp. 1890–1896.

113 J. Jaguement and J. Van Mierlo, *J. Energy Storage*, 2020, **31**, 101551.

114 B. Chidambaranathan, M. Vijayaram, V. Suriya, R. Sai Ganesh and S. Soundarraj, *Mater. Today: Proc.*, 2020, **33**, 116–128.

115 S. Liu, T. Ma, Z. Wei, G. Bai, H. Liu, D. Xu, Z. Shan and F. Wang, *J. Energy Chem.*, 2021, **52**, 20–27.



116 A. A. H. Akinlabi and D. Solyali, *Renewable Sustainable Energy Rev.*, 2020, **125**, 109815.

117 D. Bernardi, E. Pawlikowski and J. Newman, *Electrochem. Soc. Ext. Abstr.*, 1984, **84-2**(1), 164–165.

118 C. S. Chin, Z. Gao and C. Z. Zhang, *J. Energy Storage*, 2020, **28**, 101222.

119 M. I. Ardani, M. A. Wahid, M. H. A. Talib, Z. H. C. Daud, Z. Asus and M. A. M. Ariff, *Mater. Today: Proc.*, 2020, 4–7.

120 Y. Li, Z. Zhou and W. T. Wu, *Appl. Therm. Eng.*, 2019, **147**, 829–840.

121 Y. Gan, J. Wang, J. Liang, Z. Huang and M. Hu, *Appl. Therm. Eng.*, 2020, **164**, 114523.

122 X. Hua, C. Heckel, N. Modrow, C. Zhang, A. Hales, J. Holloway, A. Jnawali, S. Li, Y. Yu, M. Loveridge, P. Shearing, Y. Patel, M. Marinescu, L. Tao and G. Offer, *eTransportation*, 2021, **7**, 100099.

123 B. Wu and W. Lu, *J. Mech. Phys. Solids*, 2019, **125**, 89–111.

124 Q. Li, Y. Wang, H. Li, C. Lian and Z. Wang, *Int. J. Energy Res.*, 2021, **45**, 3913–3928.

125 B. Liu, Y. Jia, C. Yuan, L. Wang, X. Gao, S. Yin and J. Xu, *Energy Storage Mater.*, 2020, **24**, 85–112.

126 J. M. Reniers, G. Mulder and D. A. Howey, *J. Electrochem. Soc.*, 2019, **166**, A3189–A3200.

127 A. Mallarapu, J. Kim, K. Carney, P. DuBois and S. Santhanagopalan, *eTransportation*, 2020, **4**, 100065.

128 A. Rasheed, O. San and T. Kvamsdal, *arXiv*, 2019, preprint, 1–31.

129 X. Hu, F. Feng, K. Liu, L. Zhang, J. Xie and B. Liu, *Renewable Sustainable Energy Rev.*, 2019, **114**, 109334.

130 M.-F. Ng, J. Zhao, Q. Yan, G. J. Conduit and Z. W. Seh, *Nat. Mach. Intell.*, 2020, **2**, 161–170.

131 J. Qiao, S. Wang, C. Yu, X. Yang and C. Fernandez, *Energy*, 2023, **263**, 126164.

132 Z. G. Wei, J. Hu, H. He, Y. Li and B. Xiong, *IEEE Trans. Power Electron.*, 2021, **36**(10), 10970–10975.

133 P. Saha, S. Dey and M. Khanra, *J. Power Sources*, 2019, **434**, 226696.

134 M. S. Ahmed, S. A. Raihan and B. Balasingam, *Appl. Energy*, 2020, **267**, 114880.

135 P. Shrivastava, T. K. Soon, M. Y. I. Bin Idris and S. Mekhilef, *Renewable Sustainable Energy Rev.*, 2019, **113**, 109233.

136 Z. Wang, D. T. Gladwin, M. J. Smith and S. Haass, *Appl. Energy*, 2021, **294**, 117022.

137 D. Sun, X. Yu, C. Zhang, C. Wang and R. Huang, *Int. J. Energy Res.*, 2020, **44**, 11199–11218.

138 W. Yan, B. Zhang, G. Zhao, S. Tang, G. Niu and X. Wang, *IEEE Trans. Ind. Electron.*, 2019, **66**, 3227–3236.

139 J. Zhengxin, S. Qin, W. Yujiang, W. Hanlin, G. Bingzhao and H. Lin, *Energy*, 2021, **230**, 120805.

140 X. Shu, G. Li, J. Shen, W. Yan, Z. Chen and Y. Liu, *J. Power Sources*, 2020, **462**, 228132.

141 C. Sun, H. Lin, H. Cai, M. Gao, C. Zhu and Z. He, *Electrochim. Acta*, 2021, **387**, 138501.

142 Y. Fang, Q. Zhang, H. Zhang, W. Xu, L. Wang, X. Shen, F. Yun, Y. Cui, L. Wang and X. Zhang, *IET Power Electron.*, 2021, **14**, 1515–1528.

143 D. Kong, S. Wang and P. Ping, *J. Energy Storage*, 2021, **44**, 103389.

144 L. Chen, S. Wang, H. Jiang, C. Fernandez and X. Xiong, *Int. J. Energy Res.*, 2021, **45**, 15481–15494.

145 I. B. Espedal, A. Jinasena, O. S. Burheim and J. J. Lamb, *Energies*, 2021, **14**, 3248.

146 S. Zhou, Z. Chen, D. Huang and T. Lin, *IEEE Trans. Power Electron.*, 2021, **36**, 13434–13448.

147 B. Rumberg, B. Epding, I. Stradtmann and A. Kwade, *J. Energy Storage*, 2019, **25**, 100890.

148 J. Olmos, I. Gandiaga, A. Saez-de-Ibarra, X. Larrea, T. Nieva and I. Aizpuru, *J. Energy Storage*, 2021, **40**, 102765.

149 H. Tian, P. Qin, K. Li and Z. Zhao, *J. Cleaner Prod.*, 2020, **261**, 120813.

150 A. Yang, Y. Wang, F. Yang, D. Wang, Y. Zi, K. L. Tsui and B. Zhang, *J. Power Sources*, 2019, **443**, 227108.

151 X. Zhu, R. I. Revilla, J. Jaguemont, J. Van Mierlo and A. Hubin, *J. Phys. Chem. C*, 2019, **123**, 30046–30058.

152 D. Galatro, C. Da Silva, D. A. Romero, O. Trescases and C. H. Amon, *Int. J. Energy Res.*, 2020, **44**, 3954–3975.

153 M. Naumann, F. Spingler and A. Jossen, *J. Power Sources*, 2020, **451**, 227666.

154 S. Khaleghi Rahimian, M. M. Forouzan, S. Han and Y. Tang, *Electrochim. Acta*, 2020, **348**, 136343.

155 S. K. Rechkemmer, X. Zang, W. Zhang and O. Sawodny, *J. Energy Storage*, 2020, **30**, 101547.

156 B. Jiang, H. Dai and X. Wei, *Appl. Energy*, 2020, **269**, 115074.

157 T. Shibagaki, Y. Merla and G. J. Offer, *J. Power Sources*, 2018, **374**, 188–195.

158 X. Li, A. M. Colclasure, D. P. Finegan, D. Ren, Y. Shi, X. Feng, L. Cao, Y. Yang and K. Smith, *Electrochim. Acta*, 2019, **297**, 1109–1120.

159 J. He, X. Bian, L. Liu, Z. Wei and F. Yan, *J. Energy Storage*, 2020, **29**, 101400.

160 X. Feng, Y. Merla, C. Weng, M. Ouyang, X. He, B. Y. Liaw, S. Santhanagopalan, X. Li, P. Liu, L. Lu, X. Han, D. Ren, Y. Wang, R. Li, C. Jin, P. Huang, M. Yi, L. Wang, Y. Zhao, Y. Patel and G. Offer, *eTransportation*, 2020, **3**, 100051.

161 C. P. Lin, J. Cabrera, D. Y. W. Yu, F. Yang and K. L. Tsui, *J. Electrochem. Soc.*, 2020, **167**, 090537.

162 M. Lucu, E. Martinez-Laserna, I. Gandiaga, K. Liu, H. Camblong, W. D. Widanage and J. Marco, *J. Energy Storage*, 2020, **30**, 101409.

163 S. Barcellona and L. Piegari, *J. Energy Storage*, 2020, **29**, 101310.

164 S. H. Park, R. Tian, J. Coelho, V. Nicolosi and J. N. Coleman, *Adv. Energy Mater.*, 2019, **9**, 1–10.

165 M. S. Hosen, D. Karimi, T. Kalogiannis, A. Pirooz, J. Jaguemont, M. Berecibar and J. Van Mierlo, *J. Energy Storage*, 2020, **28**, 101265.

166 H. N. Chu, S. U. Kim, S. K. Rahimian, J. B. Siegel and C. W. Monroe, *J. Power Sources*, 2020, **453**, 227787.

167 D. Anseán, G. Baure, M. González, I. Cameán, A. B. García and M. Dubarry, *J. Power Sources*, 2020, **459**, 227882.

168 S. Xie, L. Ren, X. Yang, H. Wang, Q. Sun, X. Chen and Y. He, *J. Power Sources*, 2020, **448**, 227425.



169 J. Liu, Q. Duan, M. Ma, C. Zhao, J. Sun and Q. Wang, *J. Power Sources*, 2020, **445**, 227263.

170 A. Kriston, A. Kersys, A. Antonelli, S. Ripplinger, S. Holmstrom, S. Trischler, H. Döring and A. Pfrang, *J. Power Sources*, 2020, **454**, 227914.

171 X. Li, K. Dai, Z. Wang and W. Han, *J. Energy Storage*, 2020, **27**, 101121.

172 H. Meng and Y. F. Li, *Renewable Sustainable Energy Rev.*, 2019, **116**, 109405.

173 R. Reinhardt, I. Christodoulou, S. Gassó-Domingo and B. Amante García, *J. Environ. Manage.*, 2019, **245**, 432–446.

174 I. Mathews, B. Xu, W. He, V. Barreto, T. Buonassisi and I. M. Peters, *Appl. Energy*, 2020, **269**, 115127.

175 M. Zhu, Z. Liu, J. Li and S. X. Zhu, *Eur. J. Oper. Res.*, 2020, **283**, 365–379.

176 J. Meng, L. Cai, D. I. Stroe, J. Ma, G. Luo and R. Teodorescu, *Energy*, 2020, **206**, 118140.

177 W. Li, J. Zhu, Y. Xia, M. B. Gorji and T. Wierzbicki, *Joule*, 2019, **3**, 2703–2715.

178 I. Antonopoulos, V. Robu, B. Couraud, D. Kirli, S. Norbu, A. Kiprakis, D. Flynn, S. Elizondo-Gonzalez and S. Wattam, *Renewable Sustainable Energy Rev.*, 2020, **130**, 109899.

179 P. Fermín-Cueto, E. McTurk, M. Allerhand, E. Medina-Lopez, M. F. Anjos, J. Sylvester and G. dos Reis, *Energy AI*, 2020, **1**, 100006.

180 K. Peter and A. Jossen, *J. Energy Storage*, 2016, **6**, 125–141.

181 A. Chen, X. Zhang and Z. Zhou, *InfoMat*, 2020, **2**, 553–576.

182 X. Feng, C. Weng, X. He, X. Han, L. Lu, D. Ren and M. Ouyang, *IEEE Trans. Veh. Technol.*, 2019, **68**, 8583–8592.

183 Q. Xue, G. Li, Y. Zhang, S. Shen, Z. Chen and Y. Liu, *J. Power Sources*, 2021, **482**, 228964.

184 G. won You, S. Park and D. Oh, *Appl. Energy*, 2016, **176**, 92–103.

185 H. Gong, Y. Zou, Q. Yang, J. Fan, F. Sun and D. Goehlich, *Energy*, 2018, **150**, 901–912.

186 X. Zhao, X. Zhao, Q. Yu, Y. Ye and M. Yu, *Transp. Res. D: Transp. Environ.*, 2020, **81**, 102279.

187 Z. Chen, Q. Zhang, J. Lu and J. Bi, *Energy*, 2019, **186**, 115766.

188 Q. Song, S. Wang, W. Xu, Y. Shao and C. Fernandez, *Int. J. Electrochem. Sci.*, 2021, **16**, 1–15.

189 E. Vanem, C. B. Salucci, A. Bakdi and Ø. Å. Shei Alnes, *J. Energy Storage*, 2021, **43**, 103158.

190 W. Guo and M. He, *Appl. Soft Comput.*, 2022, **124**, 108967.

191 C. Lin, J. Xu and X. Mei, *Energy Storage Mater.*, 2023, **54**, 85–97.

192 P. Guo, Z. Cheng and L. Yang, *J. Power Sources*, 2019, **412**, 442–450.

193 P. Tagade, K. S. Hariharan, S. Ramachandran, A. Khandelwal, A. Naha, S. M. Kolake and S. H. Han, *J. Power Sources*, 2020, **445**, 227281.

194 Z. Yun, W. Qin and W. Shi, *J. Energy Storage*, 2022, **52**, 104916.

195 B. Jiang, W. E. Gent, F. Mohr, S. Das, M. D. Berliner, M. Forsuelo, H. Zhao, P. M. Attia, A. Grover, P. K. Herring, M. Z. Bazant, S. J. Harris, S. Ermon, W. C. Chueh and R. D. Braatz, *Joule*, 2021, **5**, 3187–3203.

196 P. M. Attia, A. Grover, N. Jin, K. A. Severson, T. M. Markov, Y. H. Liao, M. H. Chen, B. Cheong, N. Perkins, Z. Yang, P. K. Herring, M. Aykol, S. J. Harris, R. D. Braatz, S. Ermon and W. C. Chueh, *Nature*, 2020, **578**, 397–402.

197 H. Chun, J. Kim and S. Han, *IFAC-PapersOnLine*, 2019, **52**(4), 129–134.

198 F. Feng, S. Teng, K. Liu, J. Xie, Y. Xie, B. Liu and K. Li, *J. Power Sources*, 2020, **455**, 227935.

199 F. Yang, W. Li, C. Li and Q. Miao, *Energy*, 2019, **175**, 66–75.

200 W. Li, L. Du, W. Fan and Y. Zhu, *Int. J. Hydrogen Energy*, 2019, **44**(23), 12270–12276.

201 Y. Toughzaoui, S. B. Toosi, H. Chaoui, H. Louahlia, R. Petrone, S. Le Masson and H. Gualous, *J. Energy Storage*, 2022, **51**, 104520.

202 X. Lin and J. Zhang, *J. Energy Storage*, 2022, **46**, 103890.

203 M. Jiao, D. Wang and J. Qiu, *J. Power Sources*, 2020, **459**, 228051.

204 J. Bao, V. Murugesan, C. J. Kamp, Y. Shao, L. Yan and W. Wang, *Adv. Theory Simul.*, 2020, **3**, 1–13.

205 A. G. Kashkooli, H. Fathiannasab, Z. Mao and Z. Chen, *J. Electrochem. Soc.*, 2019, **166**, A605–A615.

206 P. Li, Z. Zhang, Q. Xiong, B. Ding, J. Hou, D. Luo, Y. Rong and S. Li, *J. Power Sources*, 2020, **459**, 228069.

207 S. Shen, M. Sadoughi, M. Li, Z. Wang and C. Hu, *Appl. Energy*, 2020, **260**, 114296.

208 X. Li, L. Zhang, Z. Wang and P. Dong, *J. Energy Storage*, 2019, **21**, 510–518.

209 C. Bian, H. He and S. Yang, *Energy*, 2020, **191**, 116538.

210 J. Hong, Z. Wang, W. Chen, L. Y. Wang and C. Qu, *J. Energy Storage*, 2020, **30**, 101459.

211 J. Hong, Z. Wang, W. Chen and Y. Yao, *Appl. Energy*, 2019, **254**, 113648.

212 E. Chemali, P. J. Kollmeyer, M. Preindl and A. Emadi, *J. Power Sources*, 2018, **400**, 242–255.

213 L. Ren, L. Zhao, S. Hong, S. Zhao, H. Wang and L. Zhang, *IEEE Access*, 2018, **6**, 50587–50598.

214 S. Khaleghi, Y. Firouz, J. Van Mierlo and P. Van den Bossche, *Appl. Energy*, 2019, **255**, 113813.

215 A. H. Ganesh and B. Xu, *Renewable Sustainable Energy Rev.*, 2022, **154**, 111833.

216 J. Chen, H. Shu, X. Tang, T. Liu and W. Wang, *Energy*, 2022, **239**, 122123.

217 X. Han, H. He, J. Wu, J. Peng and Y. Li, *Appl. Energy*, 2019, **254**, 113708.

218 M. Kim, K. Kim, J. Kim, J. Yu and S. Han, *IFAC-PapersOnLine*, 2018, **51**, 404–408.

219 Q. Zhou, J. Li, B. Shuai, H. Williams, Y. He, Z. Li, H. Xu and F. Yan, *Appl. Energy*, 2019, **255**, 113755.

220 Y. Tian, R. Lai, X. Li, L. Xiang and J. Tian, *Appl. Energy*, 2020, **265**, 114789.

221 M. Kim, H. Chun, J. Kim, K. Kim, J. Yu, T. Kim and S. Han, *Appl. Energy*, 2019, **254**, 113644.

222 D. Ansean, V. M. Garcia, M. Gonzalez, C. Blanco-Viejo, J. C. Viera, Y. F. Pulido and L. Sanchez, *IEEE Trans. Ind. Appl.*, 2019, **55**, 2992–3002.

223 M. Woody, M. Arbabzadeh, G. M. Lewis, G. A. Keoleian and A. Stefanopoulou, *J. Energy Storage*, 2020, **28**, 101231.



224 Q. Lin, J. Wang, R. Xiong, W. Shen and H. He, *Energy*, 2019, **183**, 220–234.

225 W. Li, N. Sengupta, P. Dechent, D. Howey, A. Annaswamy and D. U. Sauer, *J. Power Sources*, 2021, **482**, 228863.

226 R. Xiong, L. Li and J. Tian, *J. Power Sources*, 2018, **405**, 18–29.

227 M. Lucu, E. Martinez-Laserna, I. Gandiaga and H. Camblong, *J. Power Sources*, 2018, **401**, 85–101.

228 L. Zhou, L. He, Y. Zheng, X. Lai, M. Ouyang and L. Lu, *J. Energy Storage*, 2020, **28**, 101252.

229 D. Kucevic, B. Tepe, M. Möller, P. Dotzauer, B. Schachler, A. Jossen and H. Hesse, *Open Energy Modelling Workshop 2020*, 2020, vol. 4072.

230 K. M. Alam and A. El Saddik, *IEEE Access*, 2017, **5**, 2050–2062.

